



Naval Surface Warfare Center

Carderock Division

West Bethesda, MD 20817-5700

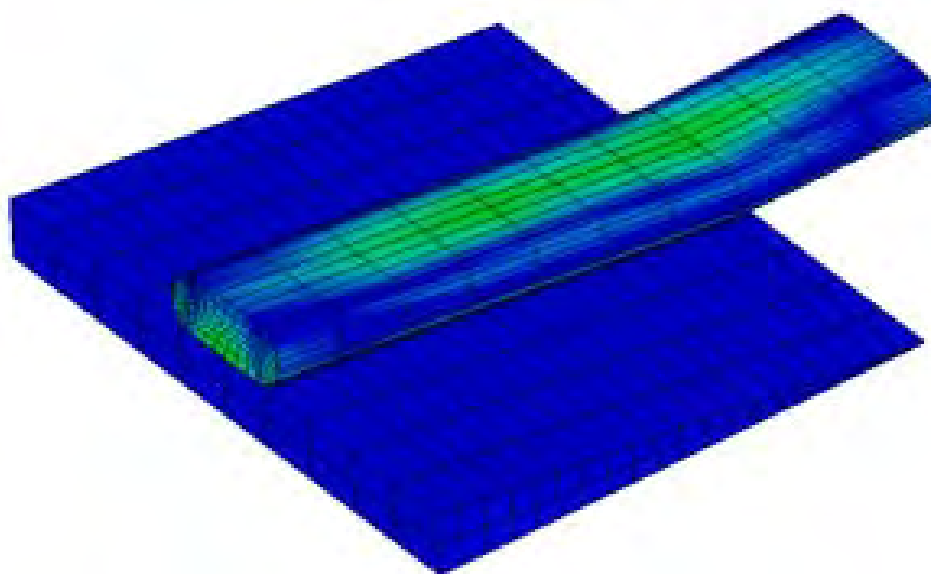
NSWCCD-CISD-2010/018 February 2011

Center for Innovation in Ship Design

Technical Report

A Feasibility Study on Numerical Modeling of Large-Scale Naval Fluid-Filled Structure: Contact-Impact Problems

By
Solomon Yim



NSWCCD-CISD-2010/018



DISTRIBUTION STATEMENT A: Approved for public release; distribution is unlimited

REPORT DOCUMENTATION PAGE				Form Approved OMB No. 0704-0188	
Public reporting burden for this collection of information is estimated to average 1 hour per response, including the time for reviewing instructions, searching existing data sources, gathering and maintaining the data needed, and completing and reviewing this collection of information. Send comments regarding this burden estimate or any other aspect of this collection of information, including suggestions for reducing this burden to Department of Defense, Washington Headquarters Services, Directorate for Information Operations and Reports (0704-0188), 1215 Jefferson Davis Highway, Suite 1204, Arlington, VA 22202-4302. Respondents should be aware that notwithstanding any other provision of law, no person shall be subject to any penalty for failing to comply with a collection of information if it does not display a currently valid OMB control number. PLEASE DO NOT RETURN YOUR FORM TO THE ABOVE ADDRESS.					
1. REPORT DATE (DD-MM-YYYY) 04-02-2011		2. REPORT TYPE Final		3. DATES COVERED (From - To) 01-06-2010 – 01-08-2010	
4. TITLE AND SUBTITLE A Feasibility Study on Numerical Modeling of Large-Scale Naval Fluid-Filled Structure: Contact-Impact Problems				5a. CONTRACT NUMBER	
				5b. GRANT NUMBER	
				5c. PROGRAM ELEMENT NUMBER	
6. AUTHOR(S) Solomon Yim				5d. PROJECT NUMBER	
				5e. TASK NUMBER	
				5f. WORK UNIT NUMBER	
7. PERFORMING ORGANIZATION NAME(S) AND ADDRESS(ES) AND ADDRESS(ES) Naval Surface Warfare Center Carderock Division 9500 MacArthur Boulevard West Bethesda, MD 20817-5700				8. PERFORMING ORGANIZATION REPORT NUMBER NSWCCD-CISD-2011/018	
9. SPONSORING / MONITORING AGENCY NAME(S) AND ADDRESS(ES) Chief of Naval Research One Liberty Center 875 North Randolph Street, Suite 1425 Arlington, VA 22203-1995				10. SPONSOR/MONITOR'S ACRONYM(S) ONR	
				11. SPONSOR/MONITOR'S REPORT NUMBER(S)	
12. DISTRIBUTION / AVAILABILITY STATEMENT DISTRIBUTION STATEMENT A: Approved for public release; distribution is unlimited					
13. SUPPLEMENTARY NOTES					
14. ABSTRACT Modeling and testing of inflatable membrane structures for rapidly deployable port infrastructures is of interest to the US Navy's new capabilities development. For decades, the Navy has used small displacement landing craft to be the conduit between heavy-tonnage ships offshore and the landing zone ashore. This has been a means of transporting troops and their combat and logistics support. A problem with this procedure is that displacement landing craft can only get close enough to the beach to disembark vehicles and personnel to wade the final distance ashore. Although the water is shallow, the vehicles need to be designed to operate in a corrosive seawater environment. An alternative method the Navy considers is floating causeways. The major objective of this study is to assess the feasibility of using an advanced numerical code to simulate the dynamics of a mobile support platform for the deployment, retrieval, and operation of the MOSES inflatable causeway under wave action. This is achieved by developing a numerical model of the wave basin with wave generation over a rigid basin bottom to study the dynamic behavior of MOSES under laboratory conditions. The purpose of this study is to compare qualitatively the numerical predictions with experimental results obtained in the experimental study to assess the feasibility of such modeling.					
15. SUBJECT TERMS Inflatable causeway, CISD, hydro-elastic model, wave basin, numerical model, large-scale fluid filled structure, naval					
16. SECURITY CLASSIFICATION OF:			17. LIMITATION OF ABSTRACT SAR	18. NUMBER OF PAGES 63	19a. NAME OF RESPONSIBLE PERSON Colen Kennell
a. REPORT UNCLASSIFIED	b. ABSTRACT UNCLASSIFIED	c. THIS PAGE UNCLASSIFIED			19b. TELEPHONE NUMBER (include area code) 301-227-5468



Abstract

Modeling and testing of inflatable membrane structures for rapidly deployable port infrastructures is of interest to the US Navy's new capabilities development. For decades, the Navy has used small displacement landing craft to be the conduit between heavy-tonnage ships offshore and the landing zone ashore. This has been a means of transporting troops and their combat and logistics support. A problem with this procedure is that displacement landing craft can only get close enough to the beach to disembark vehicles and personnel to wade the final distance ashore. Although the water is shallow, the vehicles need to be designed to operate in a corrosive seawater environment. An alternative method the Navy considers is floating causeways.

The major objective of this study is to assess the feasibility of using an advanced numerical code to simulate the dynamics of a mobile support platform for the deployment, retrieval, and operation of the MOSES inflatable causeway under wave action. This is achieved by developing a numerical model of the wave basin with wave generation over a rigid basin bottom to study the dynamic behavior of MOSES under laboratory conditions. The purpose of this study is to compare qualitatively the numerical predictions with experimental results obtained in the experimental study to assess the feasibility of such modeling.

Acknowledgments

This report is the combination of the work performed by undergraduate students from a number of universities across United States which was supported by a naval summer research program. The students were hired under the National Research Enterprise Intern Program sponsored by the Office of Naval Research. This program provides an opportunity for students to participate in research at a Department of Navy laboratory for 10 weeks during the summer. The goals of the program are to encourage participating students to pursue science and engineering careers, to further education via mentoring by laboratory personnel and their participation in research, and to make them aware of Navy research and technology efforts, which can lead to future employment. The author participated under ONR's Visiting Professor Program.

At the Naval Surface Warfare Center Carderock Division, the single largest employer of summer interns is the Center for Innovation in Ship Design (CISD), which is part of the Ship Systems Integration and Design Department. The intern program is just one way in which CISD fulfills its role of conducting student outreach and developing ship designers.

The student team consisted of:

Andrew Bloxom



Abel Medellin



Chris Vince



The team would like to acknowledge:

Steven Ouimette, Mr. Benjamin Testerman, Dr. Pat Hudson, Dr. Colen Kennell, Jack Offutt and Marty Irvine for their suggestions and support.



Executive Summary

MOSES is a conceptual inflatable causeway system designed to provide access for shallow draft vessels near the shore to the beach and it is designed to be lightweight and easy to deploy. The large fabric membrane structure is filled with seawater and pressurized to become relatively rigid. This causeway rests on the seafloor forming a roadway about a meter above the sea surface.

The major objective of this study is to assess the feasibility of using an advanced numerical code to simulate the dynamic motion of MOSES under wave action. This is achieved by developing a numerical model of the wave basin with wave generation over a rigid basin bottom to study the dynamic behavior of MOSES under laboratory conditions. The numerical predictions were compared *qualitatively* with experimental results obtained in an accompanying experimental study. The simulations thus far utilize an Arbitrary Lagrangian and Eulerian (ALE) technique to capture the multi-physics phenomenon.

MOSES was treated as a fully rigid object and then a single flexible case was tested to observe its motion under the action of the waves. Results show that the coupled FSI numerical code can successfully capture the motion of MOSES under the severe action of waves. All the numerical test cases described above show good matching of the physics of the wave motion and the motion of the membrane structure on the movable beach and the qualitative behavior compared well with those shown in the experimental test cases. Both the numerical test cases of treating the water-filled membrane (MOSES) as rigid and fully flexible show a realistic behavior of the membrane structure motion under the action of waves.

A detailed descriptions of the numerical simulation procedure specific to the modeling the physical wave basin and water-filled membrane (MOSES) using a multi-physics multi-scale finite-element code is also delineated. Specifically, a nine-step simulation procedure pertaining to such class of fluid-structure interaction problems are shown.



Table of Contents

Abstract.....	i
Acknowledgements.....	ii
Executive Summary.....	iii
Table of Contents.....	iv
List of Figures.....	v
List of Tables	vi
Nomenclature.....	vi
INTRODUCTION	1
Physical Modeling	1
Numerical Simulation	2
Objectives	3
SUMMARY OF PHYSICAL MODEL AND EXPERIMENT	3
MOSES Physical Model	3
Experimental Facility.....	4
Experimental Setup.....	9
NUMERICAL MODELING AND SIMULATION OF INFLATABLE CAUSEWAY	10
Fluid Models	10
NWT formulations and ALE description.....	10
Structural Models.....	12
Contact and Impact Models	12
LS-DYNA SPECIFIC MODELING PROCEDURE.....	16
PRELIMINARY SIMULATION RESULTS	16
CONCLUDING REMARKS.....	30
REFERENCES	32
APPENDIX.....	33
LS-DYNA SPECIFIC MODELING PROCEDURE.....	33
STEP 1: Modeling Wave Basin and Various Components	33
STEP 2: Material Models.....	45
STEP 3: Element/Section Properties	48
STEP 4: Assigning Material and Section properties.....	52
STEP 5: Boundary Conditions.....	53
STEP 6: Contact Definition	56
STEP 7: Defining Curves for Wavemaker Motion and Gravity.....	58
STEP 8: Application of ALE Multimaterials.....	62
STEP 9: Control Cards for ALE with Time Step allocation.....	63

List of Figures

Figure 1 Wave basin dimensions	6
Figures 2(a), 2(b) and 2(c) Orientation of movable beach and membrane structure	7
Figures 3(a), 3(b) and 3(c) Orientation of membrane structure without beach	8
Figure 4 Constant pressure reservoir to maintain constant pressure head	9
Figure 5 Back view of the wavemaker used for wave generation in the wave basin	9
Figure 6 Components of numerical wave basin.....	14
Figure 7 Isometric view of numerical wave basin	14
Figure 8 Close-up view of movable beach and membrane structure.....	15
Figure 9 Wave propagation above the rigid membrane structure (Case-I)	22
Figure 10 Wave propagation above the rigid membrane structure (Case-II)	24
Figure 11 Wave propagation above the rigid membrane structure (Case-III).....	27
Figure 12 LS-PrePost stress contour plots for a flexible membrane structure (Case-IV)	29
Figure 13 Elevation of Waver-Air domain of actual wave basin	34
Figure 14 Isometric view of actual wave basin	34
Figure 15 Elevation of water domain (2D-view).....	35
Figure 16 Elevation of air domain (2D-view).....	36
Figure 17 Elevation of air and water domain (2D-view).....	37
Figure 18 Isometric view of air and water domains (3D).....	37
Figure 19 Transparent view of air and water domains	38
Figure 20 Isometric view of face of wavemaker and front view of water domain	39
Figure 21 Vector normals of wavemaker in line with water domain	39
Figure 22 Movable Beach.....	40
Figure 23 Membrane structure and movable beach.....	41
Figure 24 Complete assembly of air, water, wavemaker, beach and membrane structure.....	41
Figure 25 Up-close of complete assembly (view from the wavemaker side).....	42
Figure 26 Up-close of springs attached to membrane structure	43
Figure 27 Isometric view of movable beach and springs attached to membrane structure	44
Figure 28 Complete model information for simulation of numerical wave basin.....	44
Figure 29 Material properties for wavemaker	47
Figure 30 Material properties for springs	47
Figure 31 Section properties for water domain.....	48
Figure 32 Section properties for wavemaker	49
Figure 33 Section properties for movable beach	50
Figure 34 Section properties for defining spring elements.....	51
Figure 35 Assigning material/section/EOS data to all the parts in LS-PREPOST	52
Figure 36 Application of boundary conditions	53
Figure 37 Boundary SPC set card definition	54
Figure 38 Segment set created to define the non-reflecting BC	55
Figure 39 Non-reflecting BC card	55
Figure 40 Constrained Lagrangian in Solid card details.....	57
Figure 41 NQUAD/Normal direction of coupling between Lagrangian and Eulerian parts	57
Figure 42 Gravity loading on wave basin (Acceleration time history).....	58



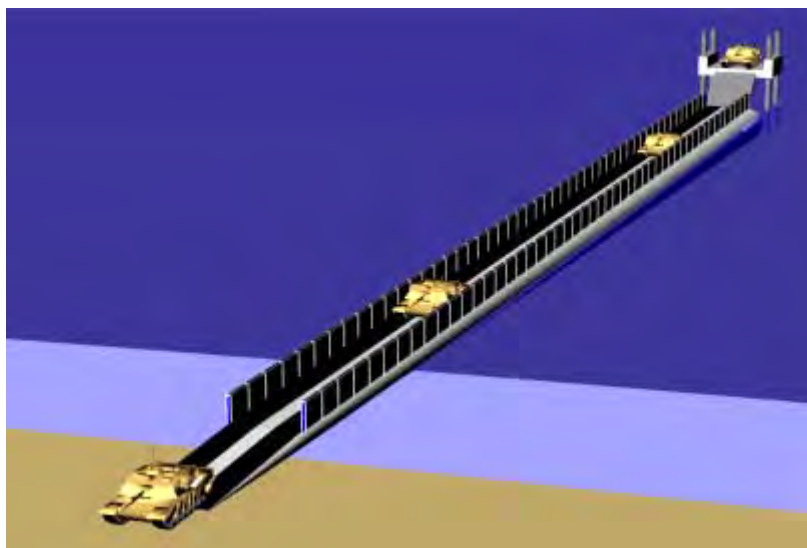
Figure 43 Wavemaker displacement time history	59
Figure 44 Load Body card to define gravity loading.....	59
Figure 45 Boundary prescribed motion rigid card for wavemaker motion	60
Figure 46 Friction between membrane structure/beach and bottom of wave basin	61
Figure 47 Multimaterial ALE card	62
Figure 48 Control ALE card details.....	63

List of Tables

Table 1: Gruniesen parameters for water.....	46
--	----

Nomenclature

SS	Sea State
NSWCCD	Naval Surface Warfare Center Carderock Division
CISD	Center for Innovation in Ship Design
MEB	Marine Expeditionary Brigade
LSTC	Livermore Software Technology Corporation
FSI	Fluid Structure Interaction
NWT	Numerical Wave Tank
ALE	Arbitrary Lagrangian Eulerian
EOS	Equation of State



INTRODUCTION

Modeling and testing of inflatable membrane structures for rapidly deployable port infrastructures is of interest to the US Navy's new capabilities development. For decades, the Navy has used small displacement landing craft to be the conduit between heavy-tonnage ships offshore and the landing zone ashore. This has been a means of transporting troops and their combat and logistics support. A problem with this procedure is that displacement landing craft can only get close enough to the beach to disembark vehicles and personnel to wade the final distance ashore. Although the water is shallow, the vehicles need to be designed to operate in a corrosive seawater environment. An alternative method the Navy considers is floating causeways.

Physical Modeling

MOSES is one such conceptual inflatable causeway system designed to provide access for shallow draft vessels near the shore to the beach. The system is designed to be lightweight and easy to deploy (Bloxom *et al* 2010). MOSES is a large fabric membrane structure filled with seawater and pressurized to become relatively rigid. This causeway rests on the seafloor forming a roadway about a meter above the sea surface. The goal of the MOSES project is to design a

causeway that can reach large ships several hundred meters from the shore, keep vehicles dry, and be operational in at least Sea State 4 (SS4) conditions. On-going research of inflatable structures shows that they can be easily deployed, lightweight and compact making them appealing.

Using the seafloor for support enables the causeway to remain stable in high sea states remaining relatively unaffected by large swells. The weight of the water in the membrane structure above sea level creates a large downward force, which holds the system in place. To minimize rolling, MOSES contains internal fabric ribs that run its entire length. These ribs create a structure with a flat bottom and top. The selected shape provides for a roadway on top and the flat bottom ensures stability against rolling. An experiment on a scaled model of MOSES was conducted in the summer of 2010 (Bloxom *et al* 2010).

Numerical Simulation

Large-scale Naval fluid structure contact-impact problems such as the conceptual inflatable causeway project form an interesting and challenging interdisciplinary area of Fluid-Structure interaction (FSI). Methods that use results from physical wave basin experiments to assess the wave forces on such structures are usually employed to investigate such class of problems. These experiments, though closer to the physical phenomena, often tend to be time-consuming and expensive and it is not economically feasible to conduct parametric studies. Alternatively, numerical models when developed with similar capabilities will complement the experiments well because of the lower costs and the ability to study phenomena that are not feasible in the laboratory. LS-DYNA is one such numerical model that is used most often to analyze this class of contact-impact problems.

LS-DYNA (developed by LSTC) is a multi-functional code with explicit and implicit finite-elements to simulate and analyze highly nonlinear physical phenomenon which usually involves large deformations within short time duration. It is an advanced nonlinear finite-element based commercially available numerical software which has arguably the best solid mechanics, contact and impact models among commercially available software, and has growing fluid mechanic features (Hallquist, 2006). The main solution methodology is based on explicit time integration. An implicit solver is currently available with somewhat limited capabilities including structural analysis and heat transfer. It also has an excellent computational framework combined with pre- and post-processing capabilities to address various research and application needs. A significant number of fluid-structure interaction models in the industry have been successfully employed using finite-element (FE) codes with an arbitrary Lagrangian-Eulerian (ALE) formulation and a

contact-impact algorithm because this code enables the modeling of the instantaneous coupling between the fluid and the structure (Hallquist, 2006).

Contact-impact algorithms have always been an important stand out capability in the LS-DYNA family of codes. Contact and impact may occur along surfaces of a single body undergoing large deformations, between two or more deformable bodies, or between a deformable body and a rigid barrier. This type of interface/contact is mainly used when there is a need for the ALE transformations for the impact scenario (specifically meant for FSI problems). By a specialization of this algorithm, such interfaces can be rigidly tied to admit variable zoning without the need of mesh transition regions (Hallquist, 2006). The purpose of the present study is to provide a preliminary assessment of an advanced numerical code in simulating complex fluid-structure interaction behaviors of the model-scale system.

Objectives

The major objective of this study is to assess the feasibility of using an advanced numerical code to simulate the dynamics of a mobile support platform for the deployment, retrieval, and operation of the MOSES inflatable causeway under wave action. This is achieved by developing a numerical model of the wave basin with wave generation over a rigid basin bottom to study the dynamic behavior of MOSES under laboratory conditions. The purpose of this study is to compare qualitatively the numerical predictions with experimental results obtained in the experimental study (Bloxom *et al* 2010) to assess the feasibility of such modeling.

SUMMARY OF PHYSICAL MODEL AND EXPERIMENT

MOSES Physical Model

MOSES is designed to be pressurized to make the system sufficiently rigid for vehicles to drive across (roll-on roll-off). The required pressure is induced through the use of reservoirs that are open to the atmosphere. The reservoirs serve two main purposes. Firstly, they raise the level of the water above the roadway, which creates a sufficient pressure head to make the MOSES rigid. Secondly, the reservoirs act as walls, deflecting the large swells expected in SS4, a design

requirement. A secondary benefit of the reservoirs is that they provide some allowance for punctures or tears in the fabric. The large reservoirs will enable the causeway to remain sufficiently rigid for several minutes after a significant puncture to allow time for safe evacuation of vehicles and personnel.

Since the system needs to be easily deployed, a simple mechanism has been designed to unroll the deflated causeway from the transport ship to the shore. Using fabric as the main structural component allows MOSES to be easily compacted and rolled around a giant spool. The recovery process is simply the reverse of the deployment process.

The viability of the MOSES causeway concept was tested using a scale model. The MOSES system is novel because of its fabric material construction, which can be compacted, stowed and easily deployed. Compared to the current causeways, MOSES has advantages in terms of deployment/recovery times, stowage volumes, and overall weight. These attributes make the inflatable causeway appealing for future development of this ship to shore transition technology. (Dickens and Rosen, 2007)

Experimental Facility

As described in Bloxom *et al* (2010) an experimental investigation of the fluid-structure interaction of water filled inflatable membrane structure in the near shore environment was performed by undergraduate students from a number of universities across United States supported by a naval summer research program (Figure 1). The structure of interest was a 10' x 2' x 0.75' tubular bag developed at the Center for Innovation in Ship Design (CISD) at the Naval Surface Warfare Center (NSWC), Carderock Division as a proof of concept for the design of a rapidly deployable inflatable structure causeway to be used either as a ship to shore connector or a breakwater.

The experiments were performed over a range of test conditions including three incident wave angles, three water depths, and a number of wave heights corresponding to various sea states. Results confirmed the previous conclusions that the bag is stable and well grounded for most operational sea conditions. Large amplitude and low frequency waves can induce significant motions of the structure, but the static and dynamic frictional coefficients between the structure and the surface in contact play a critical role in these motions. For conditions where the structure was at an angle of 45° to the incident waves, highly nonlinear wave conditions are produced which created wave over-topping and oscillatory motions of the structure.

The experimental test configuration was classified in two different categories. One that involves a beach set up and the other in the absence of a beach. Figure 2 shows the test configuration in

Center for Innovation in Ship Design

A Feasibility Study on Numerical Modeling of Large
Scale Naval Fluid Structure: Contact Impact Problems

the presence of a beach for different orientations of the beach. Similarly, Figure 3 shows the test configuration in the absence of the beach with various degrees of orientation. The dimensions of the USNA wave basin and the details of the wavemaker are summarized as follows:

- Practical water-depth range
 - 6" - 14"
- Movable beach
 - Height – 9.75"
 - Width – 96"
 - Length – 82"
 - Slope – 1:8.4
- Piston type wavemaker
 - 6" stroke max.
 - 2 Hz max.
 - Regular waves
 - Simple irregular wave spectra

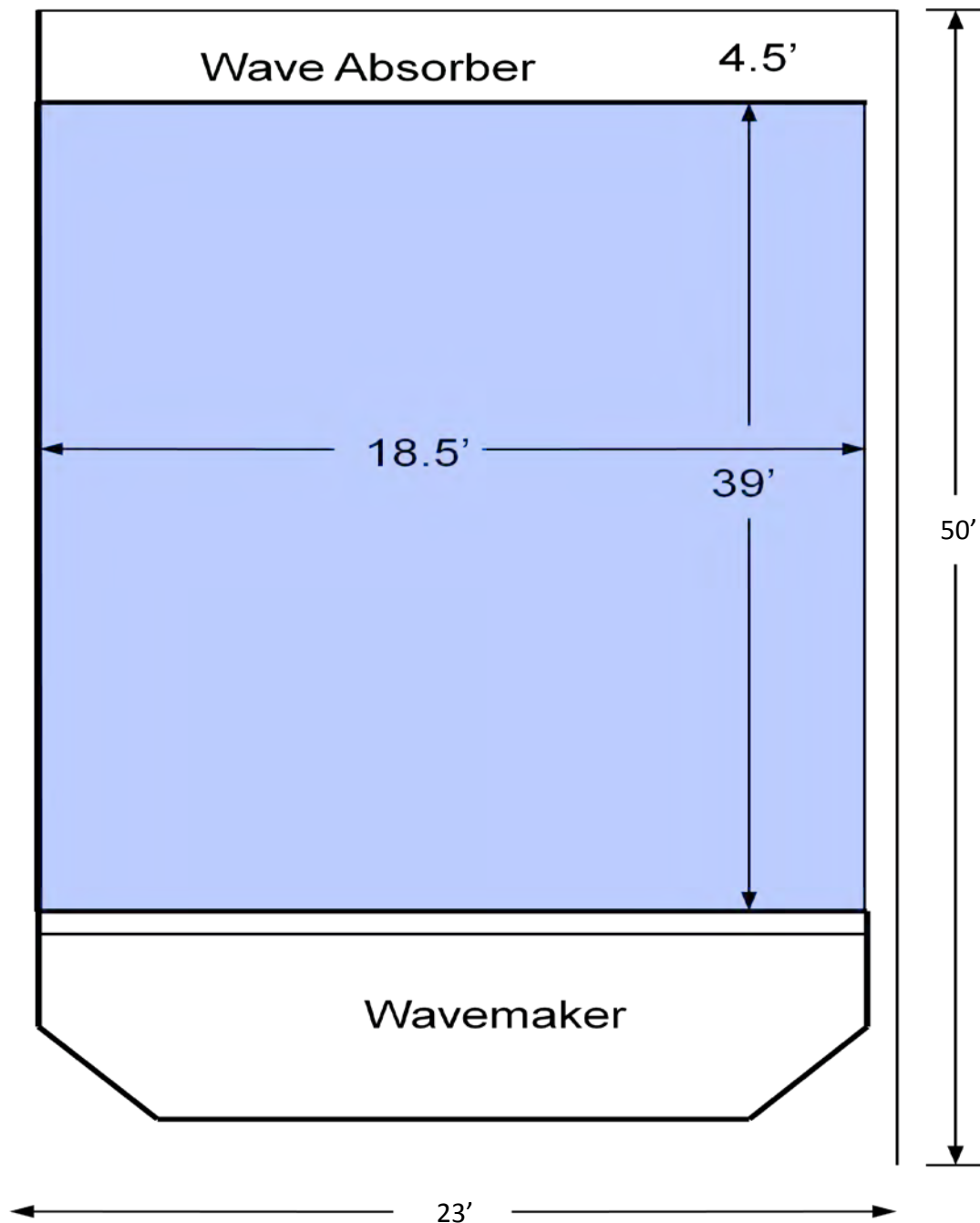
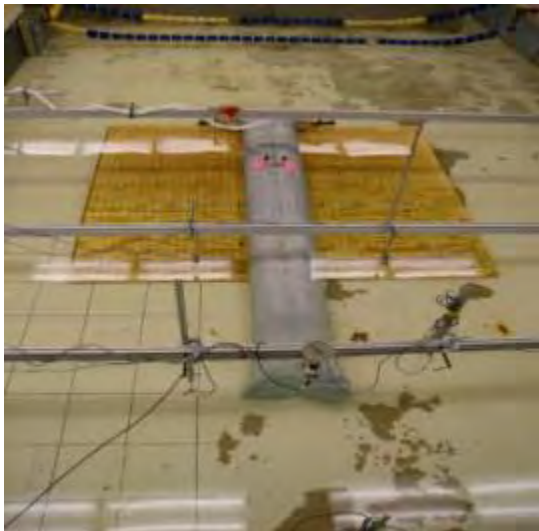


Figure 1 Wave basin dimensions

The test configuration with the removable beach is shown below.



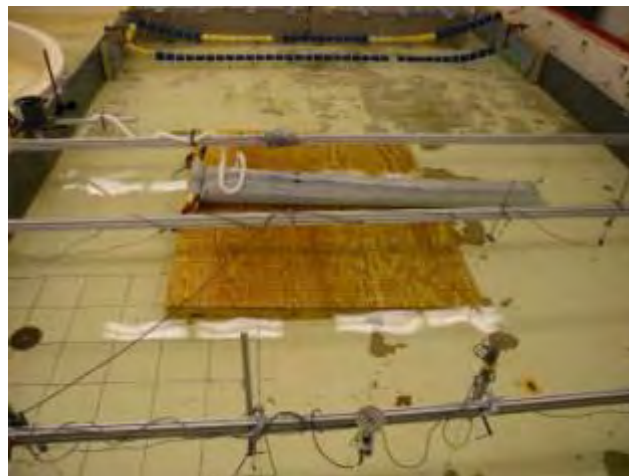
0 Degrees

Figure 2 (a)



45 Degree

Figure 2 (b)



90 Degrees

Figure 2 (c)

Figures 2(a), 2(b) and 2(c) Orientation of movable beach and membrane structure

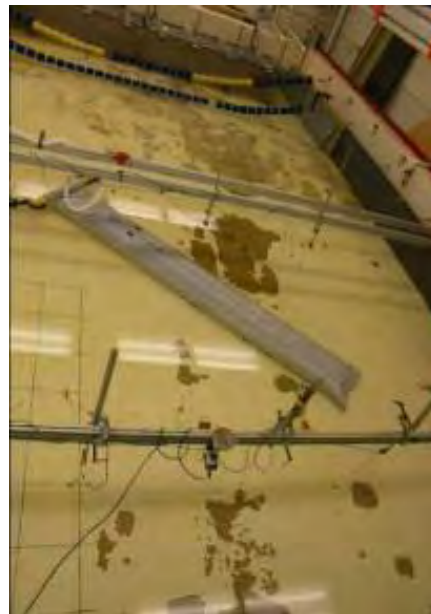
Center for Innovation in Ship Design
A Feasibility Study on Numerical Modeling of Large
Scale Naval Fluid Structure: Contact Impact Problems

The test configuration without the removable beach is shown below.



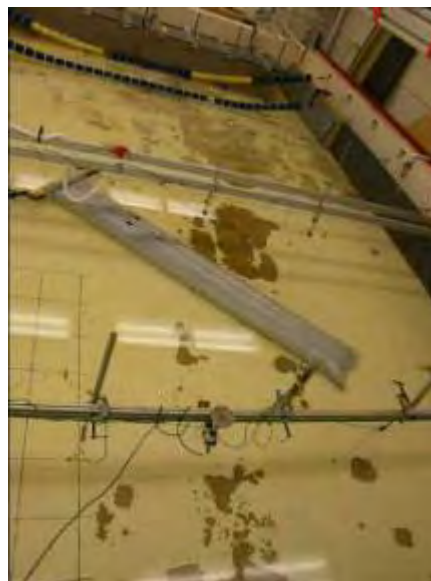
0 Degrees

Figure 3(a)



45 Degree

Figure 3(b)



90 Degree

Figure 3(c)

Figures 3(a), 3(b) and 3(c) Orientation of membrane structure without beach

Experimental Setup

The experimental and basin setup can be summarized in two figures as follows. Figure 4 shows the constant pressure reservoir to maintain constant pressure head in the membrane structure. Water was supplied steadily from one hose and overflow was drained into another one connected to the bucket. Figure 5 shows the back view of the wavemaker used for wave generation in the experimental wave basin (see Bloxom *et al* 2010 for a detailed description).

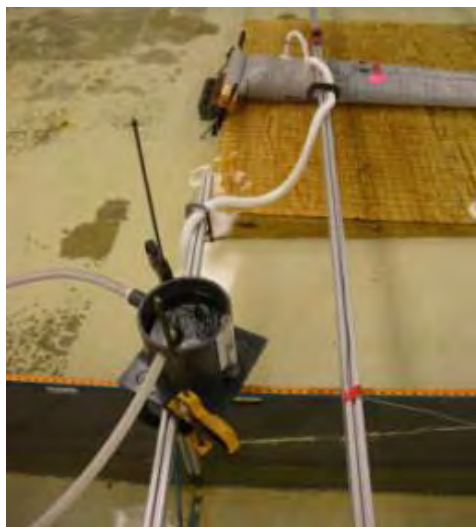


Figure 4 Constant pressure reservoir to maintain constant pressure head



Figure 5 Back view of the wavemaker used for wave generation in the wave basin

NUMERICAL MODELING AND SIMULATION OF INFLATABLE CAUSEWAY

The complexity of the experiments demands an advanced robust predictive numerical code to model the system components accurately. Numerical modeling of the MOSES inflatable causeway is carried out using a finite element code. It is a state-of-the-art nonlinear multi-physics computational mechanics code with advanced contact and impact modeling capabilities. The multi-physics feature allows the modeling of coupled fluid-structure interaction between the waves and the membrane structure and the contact and impact capability is essential for modeling the wave impact effects. The research group at Oregon State University has a long-term research collaborative relationship with Livermore Software Technology Corporation (LSTC), the software company that owns LS-DYNA.

Fluid Models

Throughout the past decade considerable progress has been made in implementing various fluid models in the numerical code. Importantly, the fluid flow solver capability is adopted to simulate the viscous flow in this project. To date these fluid models are used for different applications, varying from regular elastic and acoustic fluid elements to the complex null material model which demands an equation of state to be prescribed (Hallquist, 2006). A detailed description of the fluid constitutive models, along with their governing equations is provided in the theory manual (Hallquist, 2006). The material model parameters that can be calibrated to these data sets have only been used in the existing models. Only those fluid models whose material characterization is readily available and widely tested for these sects of problems have been used for the present FSI problem. The current fluid models are based on Navier-Stokes equation, with an arbitrary Lagrangian-Eulerian formulation. An equation of state is essential to capture the fluid behavior.

NWT formulations and ALE description

The water domain in the Numerical Wave Tank (NWT) is governed by the compressible Navier-Stokes equations and solved numerically using an ALE formulation over the entire domain.

$$\begin{aligned} \frac{D\rho}{Dt} + \rho \nabla \cdot \vec{u} &= 0 \\ \frac{D\vec{u}}{Dt} + \vec{u} \cdot \nabla \vec{u} &= -\frac{1}{\rho} (\nabla P + \frac{2}{3} \mu \nabla \cdot \vec{u}) + \frac{\mu}{\rho} \nabla^2 \vec{u} + \vec{g} \end{aligned} \quad (1)$$

where ρ is the fluid density, \vec{u} is the water particle velocity, μ is the bulk viscosity and g is the body force due to gravity. Figure 16 shows the computation domain of the NWT with the FE-ALE mesh (Appendix).

Simulations involving the NWT are often demanding because of the large distortions of the fluid elements and there is always a need to track the water (unsteady) free surface precisely. The ALE formulation takes advantage of two classical descriptions of motion: Lagrangian and Eulerian. The Lagrangian description is mainly employed in structural mechanics because of its excellent capability in tracking free surfaces and interfaces between different materials. On the other hand, the Eulerian description is widely used in computational fluid dynamics because it can efficiently handle large distortions due to fluid particles movements. The ALE formulation can be thought of as an algorithm consisted of a Lagrangian time step followed by a remap step. The remap step stops the calculation when the mesh is distorted. It then smoothes the mesh, and remaps the solution from the distorted mesh to the smoothed mesh (Belytschko et al 1982).

In theory, the Eulerian description is a subset in the ALE formulation. Early ALE formulations were not able to smooth the mesh successfully while most of the difficulties have been conquered by associating the mesh with the nodes on the material boundaries. The ALE differential form of the conservation equations for mass, momentum, and energy are readily obtained from the corresponding Eulerian forms (Belytschko et al 1982):

$$\text{Mass:} \quad \frac{d\rho}{dt} = \frac{\partial \rho}{\partial t} \Big|_x + c \cdot \nabla \rho = -\rho \nabla \cdot v \quad (2)$$

$$\text{Momentum:} \quad \rho \frac{dv}{dt} = \rho \left(\frac{\partial v}{\partial t} \Big|_x + (c \cdot \nabla) v \right) = \nabla \cdot \sigma + \rho b \quad (3)$$

$$\text{Energy:} \quad \rho \frac{dE}{dt} = \rho \left(\frac{\partial E}{\partial t} \Big|_x + c \cdot \nabla E \right) = \nabla \cdot (\sigma \cdot v) + v \cdot \rho b \quad (4)$$

Where ρ is the mass density, v is the material velocity vector, σ denotes the Cauchy stress tensor, b is the specific body force vector, E is the specific total energy, and c is the convective velocity $c = v - \hat{v}$, where \hat{v} is the grid velocity.

The numerical wave tank ideally has a non-reflective boundary condition at the far end of the solution domain in order to absorb the wave energy and prevent reflection but for the present purpose a reflecting-type boundary is used on the far end of the NWT to obtain the motion of the mine under a reflective wave. The other boundaries of the solution domain are along the side walls of the tank (impermeable no-slip boundary).

Structural Models

The code has a wide range of material and equation of state models, each with a unique number of history variables. There are approximately 100 material models which can be implemented according to the complexity of the problem (Hallquist, 2006). Spatial discretization is achieved by the use of four node tetrahedron and eight node solid elements, two node beam elements, three and four node shell elements, eight node solid shell elements, truss elements, membrane elements, discrete elements, and rigid bodies. It also has a wide variety of element formulations for each element type. Specialized capabilities for airbags, sensors, and seatbelts have tailored the code for applications in the automotive industry. Currently the code contains approximately one-hundred constitutive models and ten equations-of-state to cover a wide range of material behavior. A theoretical manual has been written to provide users and potential users with insight into the mathematical and physical basis of the code (Hallquist, 2006).

Contact and Impact Models

To enable flexibility for the user in modeling contact, the advanced numerical code presents a number of contact types and a number of parameters that control various aspects of the contact and impact treatment. Contact treatment forms an integral part of many large-deformation problems. Accurate modeling of contact interfaces between bodies is crucial to the prediction capability of the finite element simulations. It also offers a large number of contact types. Some types are for specific applications, and others are suitable for more general use. A contact is defined by identifying (via parts, part sets, segment sets, and/or node sets) what locations are to be checked for potential penetration of a slave node through a master segment. A search for penetrations, using any number of different algorithms, is made every time step. Though

Center for Innovation in Ship Design
A Feasibility Study on Numerical Modeling of Large
Scale Naval Fluid Structure: Contact Impact Problems

sometimes it is convenient and effective to define a single contact that will handle any potential contact situation in a model, it is permissible to define any number of contacts in a single model (Hallquist, 2006).

In a typical FSI problem, the deformations can be very large and predetermination of the contact is essential. Contact options that are available are: (i) One-way treatment of contact (ii) Two-way treatment of contact (iii) Tied contact (translational and rotational DOF, with and without failure, with and without offset) (iv) Single surface.

There are several contact-related parameters in that can be used to modify or, in many cases, improve contact behavior. Some of the contact parameters that can be used pertaining to the test cases are (i) Thickness offsets, SLTHK (ii) Shell thickness offset recommendations (iii) Contact sliding friction, FS and FD (iv) Penalty scale factors, SFS and SFM (v) Contact thickness SST and MST (vi) Viscous damping and most importantly (vii) Bucket-sort frequency, BSORT which refers to a very effective method of contact searching method to identify potential master contact segments for any given slave nodes. The Bucket-sorting is an expensive part of the contact algorithm so the number of bucket sorts should be kept to a minimum to reduce runtime. BSORT specifies the number of time steps between bucket sorts. If two relatively smooth simply-connected surfaces are moving across each other without folds, the bucket sorting has to be done at larger intervals. In certain contact scenarios where contacting parts are moving relative to each other in a rapid fashion, such as airbag deployment, more frequent (than default) bucket sorting intervals improves the contact and impact behavior (Hallquist, 2006).

The scaled model for the wave basin-actual dimensions of the movable beach and the membrane structure (Figure 6) shows various components of the numerical wave basin including a wavemaker, movable beach and MOSES (membrane structure containing internal fluid – water in this case). The water domain and the air domain form an essential component of a typical FSI model. The air domain (with zero density) is needed to capture the free surface of the water. Figure 7 shows an isometric view of the numerical wave basin and Figure 8 shows a close-up view of the movable beach and the membrane structure set-up.

Center for Innovation in Ship Design
A Feasibility Study on Numerical Modeling of Large
: Contact Impact Problems

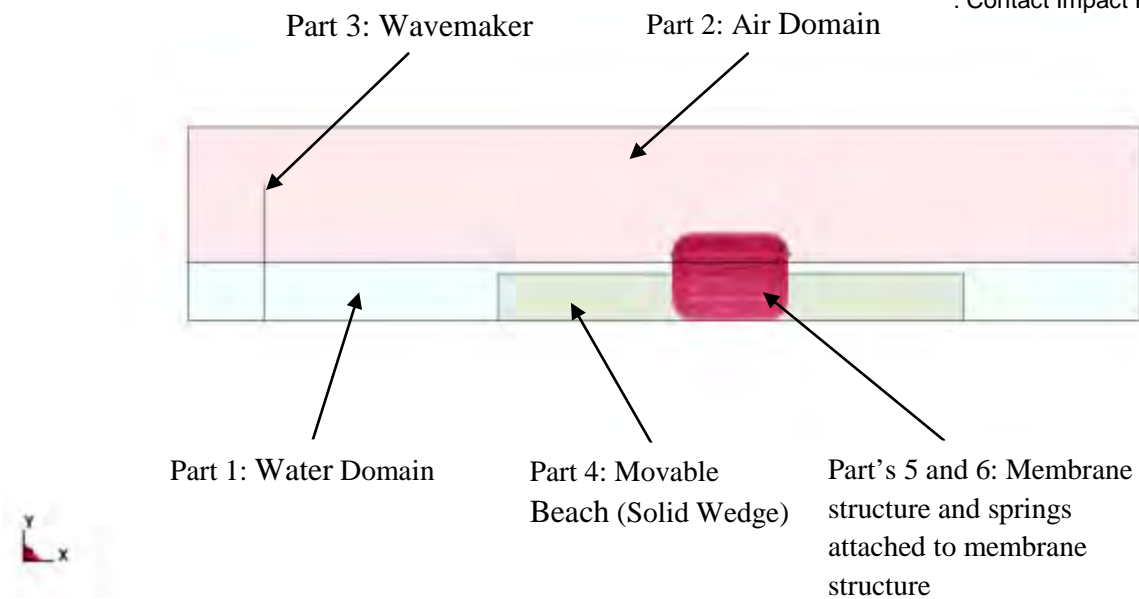


Figure 6 Components of numerical wave basin

LS-DYNA keyword deck by LS-PrePost

Flexible springs

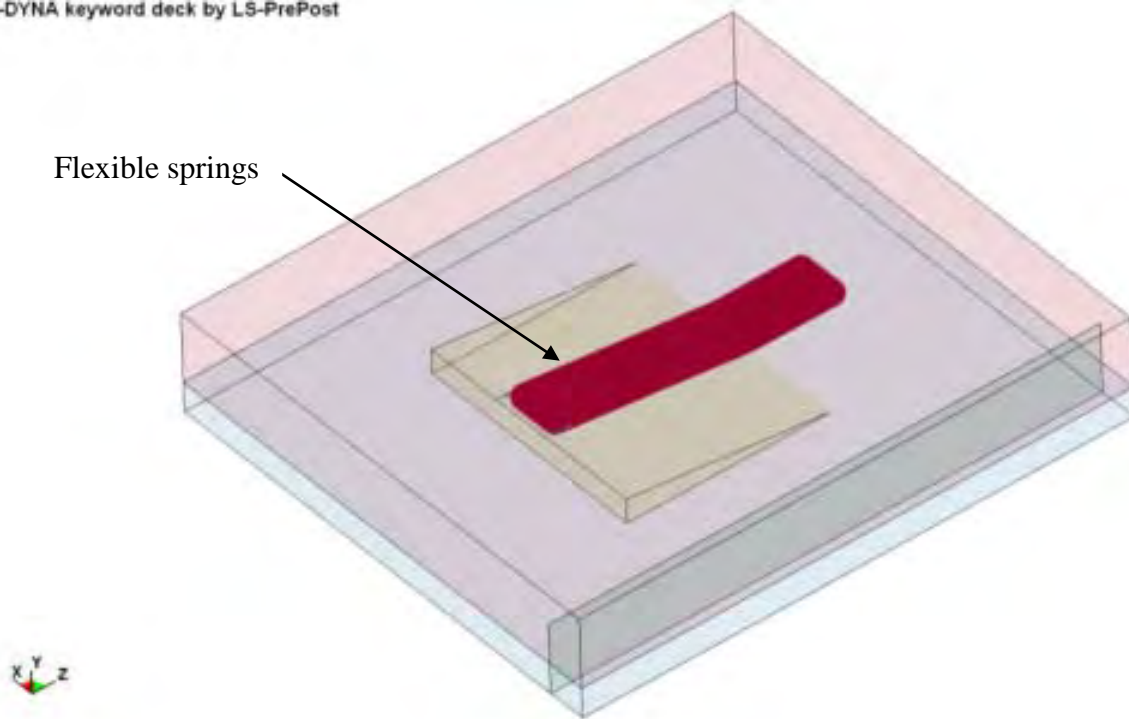


Figure 7 Isometric view of numerical wave basin

LS-DYNA keyword deck by LS-PrePost

Movable
Beach and Membrane
Structure

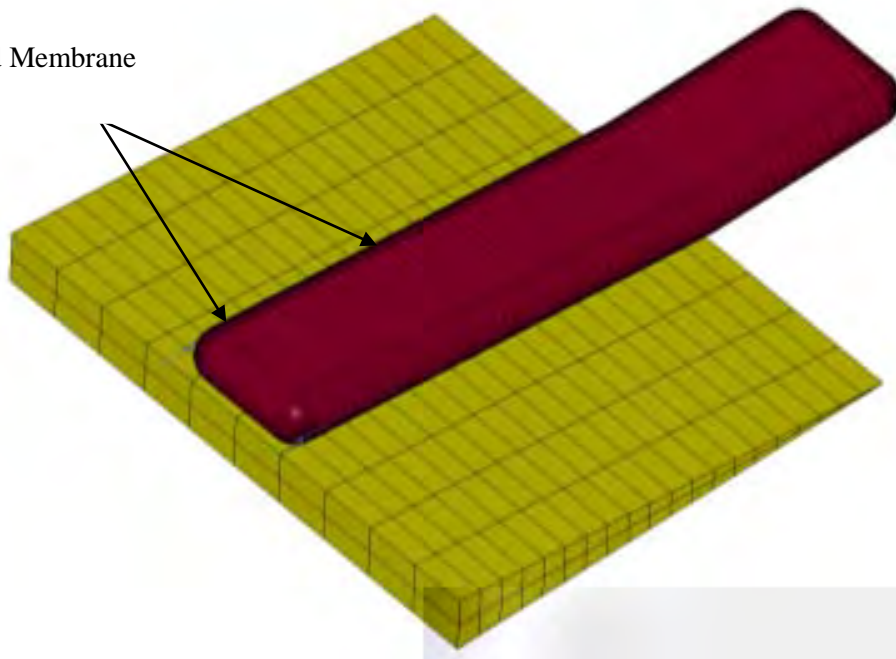


Figure 8 Close-up view of movable beach and membrane structure

The different parts that are used in modeling the numerical wave basin are listed below. The units of measurement used to build the geometry and for the analysis are N, m, kg and sec (SI).

1. Water Domain:

Material: Null Hydrodynamics
Section: Solid elements (SOLID_ALE)
Equation of State: Gruniesen EOS

2. Air Domain:

Material: Vacuum (with zero density)
Section: Solid elements (SOLID_ALE)

3. Wavemaker:

Material: Rigid material
Section: Shell elements

4. Movable Beach:

Material: Rigid material
Section: Solid elements

5. Membrane Structure:

Material: Rigid material and Flexible (Material Elastic)
Section: Shell elements

6. Springs:

Material: Spring elastic

Section: Discrete elements

LS-DYNA SPECIFIC MODELING PROCEDURE

The pre-processing procedure involves nine key steps demonstrating sequentially the construction of the modeling of the numerical wave basin. The nine steps are:

STEP 1: Modeling Wave Basin and Various Components

STEP 2: Material Models

STEP 3: Element/Section Properties

STEP 4: Assigning Material and Section properties

STEP 5: Boundary Conditions

STEP 6: Contact Definition

STEP 7: Defining Curves for Wavemaker Motion and Gravity

STEP 8: Application of ALE Multimaterials

STEP 9: Control Cards for ALE with Time Step allocation

Note: A detailed description of the sequential steps along with material and section properties will be discussed later in the Appendix section.

PRELIMINARY SIMULATION RESULTS

Numerical simulations were conducted for 15sec (model time). The models were tested with available material characterization for the air-water domain and the membrane structure. Results shown here are the sequential evolutions of the modeling of the wave basin. The results have been classified into four different cases. Each case is designed to validate specific features of the numerical model with increasing level of complexity in order to validate each modeling component to capture the real physics of the experiment.

Case-I shows the behavior of the membrane structure under the action of waves generated in the NWB with a reflective wave. Case-II shows the improvements made to Case-I by introducing a non-reflective BC and added friction between the membrane structure and the beach.

Plots shown here are the d3plot output files captures using a screen dump from LS-PrePost. The time taken to run Case-I, II and III varied from 12 to 48 hours on 10 CPUs on the Oregon State Universities College of Engineering clusters.

An isolated case of the membrane structure treated as flexible is shown in Case-IV. The termination time for this case was 10sec and the job ran on a Naval computer network on 40 nodes (CPUs) for approximately 4 days.

Case-I

The membrane structure in this case is treated as rigid ($K=5000\text{N/m}$ with added weight to the nodes where the springs are located). The stroke of the wavemaker is 0.1524m . The wave reflects back from the far end of the wave basin. Friction between the membrane structure and the beach was neglected. Figure 45 shows the wave propagation above the membrane structure in the wave basin.

LS-DYNA keyword deck by LS-PrePost
Time = 2.2493



Center for Innovation in Ship Design
A Feasibility Study on Numerical Modeling of Large
Scale Naval Fluid Structure: Contact Impact Problems

LS-DYNA keyword deck by LS-PrePost
Time = 3.1245

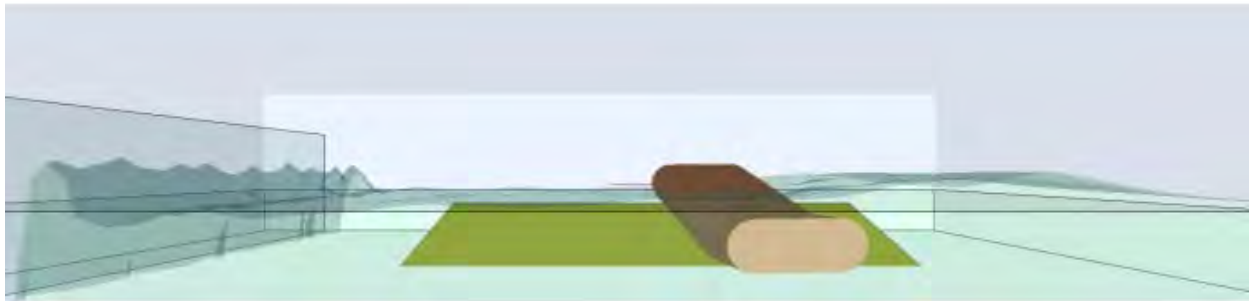


LS-DYNA keyword deck by LS-PrePost
Time = 4.8748



Center for Innovation in Ship Design
A Feasibility Study on Numerical Modeling of Large
Scale Naval Fluid Structure: Contact Impact Problems

LS-DYNA keyword deck by LS-PrePost
Time = 5.1496



LS-DYNA keyword deck by LS-PrePost
Time = 6.8743



Center for Innovation in Ship Design
A Feasibility Study on Numerical Modeling of Large
Scale Naval Fluid Structure: Contact Impact Problems

LS-DYNA keyword deck by LS-PrePost
Time = 9.2993



LS-DYNA keyword deck by LS-PrePost
Time = 9.9998



Center for Innovation in Ship Design
A Feasibility Study on Numerical Modeling of Large
Scale Naval Fluid Structure: Contact Impact Problems

LS-DYNA keyword deck by LS-PrePost
Time = 11.725



LS-DYNA keyword deck by LS-PrePost
Time = 13.274



LS-DYNA keyword deck by LS-PrePost
Time = 15



Figure 9 Wave propagation above the rigid membrane structure (Case-I)

Case-II

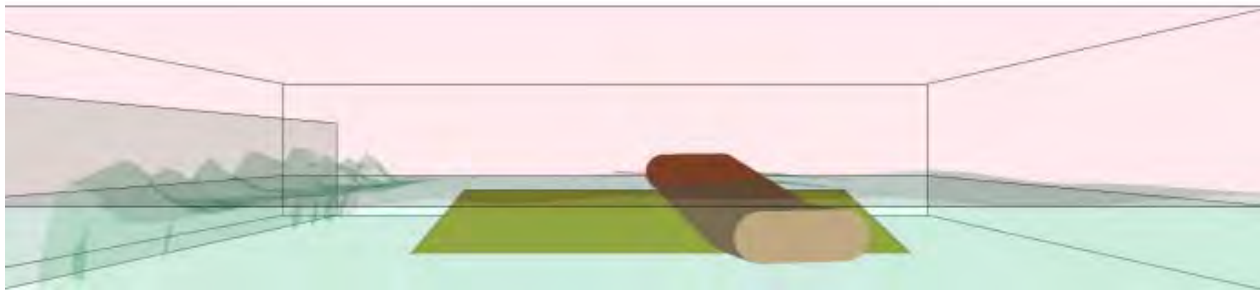
In this case, the membrane structure is also treated as rigid ($K=5000\text{N/m}$ with added weight to the nodes where the springs are located). The stroke of the wavemaker is 0.1524m . The above case had a reflecting boundary but the present case has a non-reflecting boundary with friction considered between the beach and membrane structure. As expected, the wave reflects back from the far end of the wave basin, which confirms the reflecting feature of Case-I. Figure 46 shows the wave propagation above the membrane structure for the present case.

Center for Innovation in Ship Design
A Feasibility Study on Numerical Modeling of Large
Scale Naval Fluid Structure: Contact Impact Problems

LS-DYNA keyword deck by LS-PrePost
Time = 3.3496



LS-DYNA keyword deck by LS-PrePost
Time = 5.8242



Center for Innovation in Ship Design
A Feasibility Study on Numerical Modeling of Large
Scale Naval Fluid Structure: Contact Impact Problems

LS-DYNA keyword deck by LS-PrePost
Time = 8.2404



LS-DYNA keyword deck by LS-PrePost
Time = 10.424



LS-DYNA keyword deck by LS-PrePost
Time = 12.375



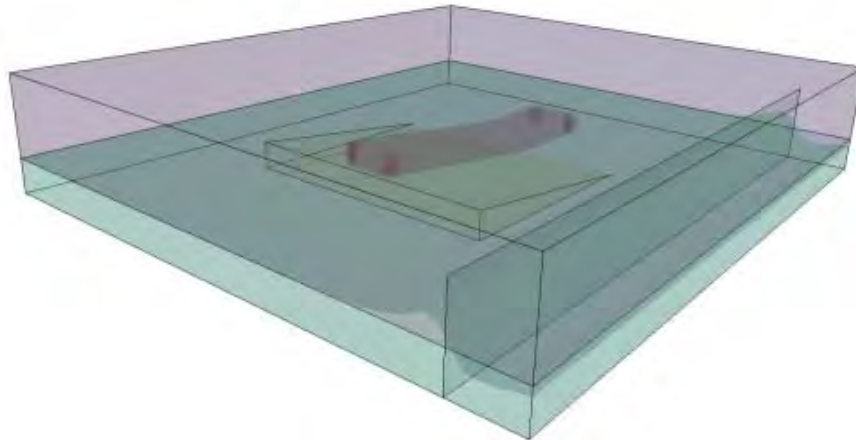
Figure 10 Wave propagation above the rigid membrane structure (Case-II)

Case-III: Test Cases with Real Shape of the membrane structure

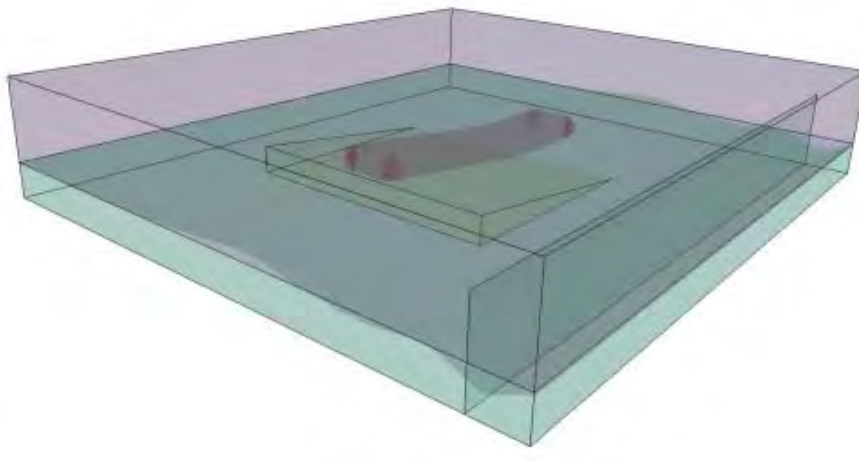
The membrane structure in this case has the actual shape and dimensions used in the experiment (treated as a rigid body). Importantly for the present case the wavemaker has a stroke of 0.0762m and a frequency of 1Hz. The spring constant is same as used for the previous working cases ($K=10,000\text{N/m}$ with added weight to the nodes 10kg each). Figure 47 shows the wave propagation above the membrane structure for Case-III. Note the wave propagation at the left edge of the wavemaker/water domain.

Center for Innovation in Ship Design
A Feasibility Study on Numerical Modeling of Large
Scale Naval Fluid Structure: Contact Impact Problems

LS-DYNA keyword deck by LS-PrePost
Time = 2.1998

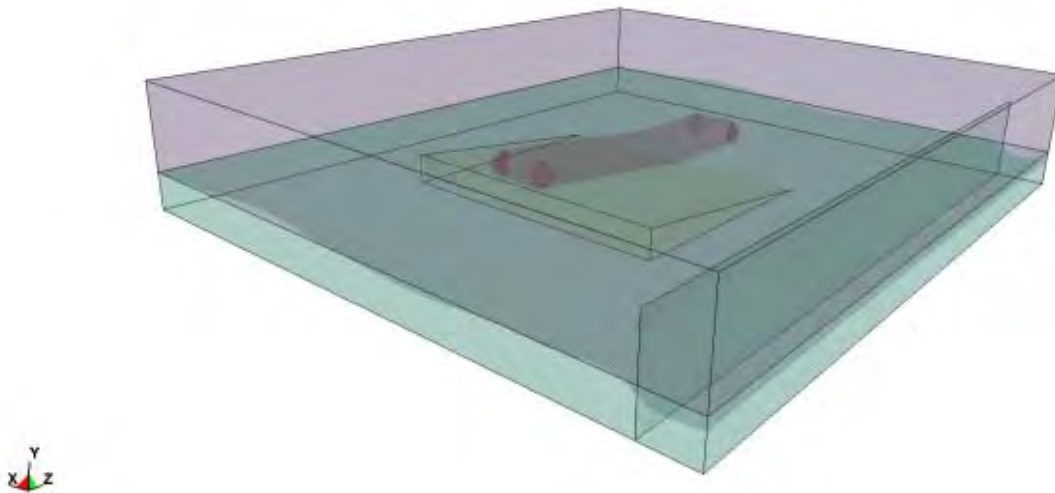


LS-DYNA keyword deck by LS-PrePost
Time = 3.0993



Center for Innovation in Ship Design
A Feasibility Study on Numerical Modeling of Large
Scale Naval Fluid Structure: Contact Impact Problems

LS-DYNA keyword deck by LS-PrePost
Time = 3.8248



LS-DYNA keyword deck by LS-PrePost
Time = 5.0749

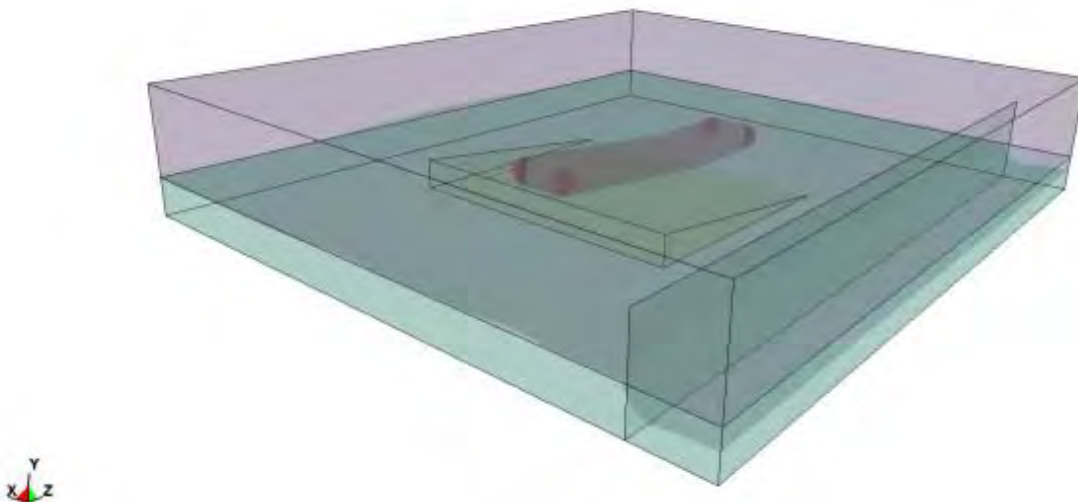
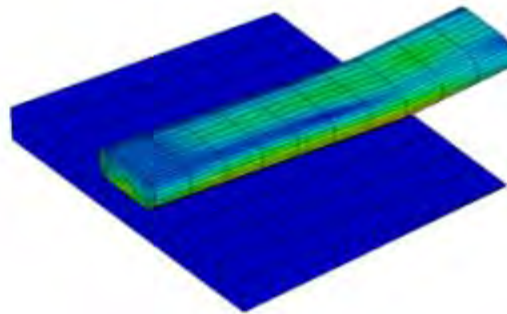


Figure 11 Wave propagation above the rigid membrane structure (Case-III)

Case-IV: Flexible test case

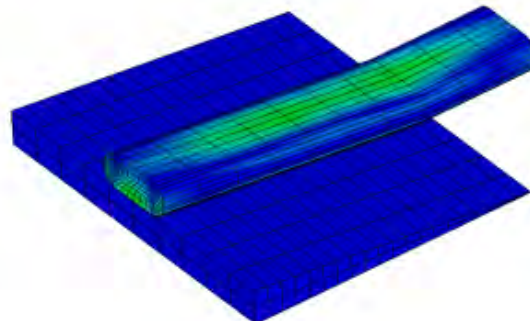
The membrane structure in this case is treated as fully elastic (Material_Elastic) with shell elements with the rest of the parameters remaining same as in previous cases. The von-Mises Stress contours on the membrane structure are shown at different times of the simulation. Figure 48 shows the stress contours plotted using the LS-PrePost on the flexible membrane structure.

LS-DYNA keyword deck by LS-PrePost
Time = 0.225
Contours of Effective Stress (v-m)
max ipt. value
min=0, at elem# 28001
max=212763, at elem# 34794



Fringe Levels
2.128e+05
1.915e+05
1.702e+05
1.489e+05
1.277e+05
1.064e+05
8.511e+04
6.383e+04
4.255e+04
2.128e+04
0.000e+00

LS-DYNA keyword deck by LS-PrePost
Time = 0.15
Contours of X-stress
max ipt. value
min=0, at elem# 28001
max=128091, at elem# 34794

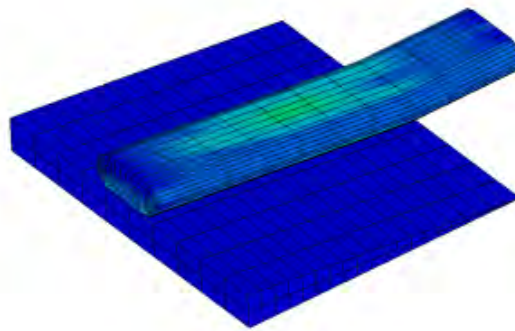


Fringe Levels
1.281e+05
1.153e+05
1.025e+05
8.966e+04
7.685e+04
6.405e+04
5.124e+04
3.843e+04
2.562e+04
1.281e+04
0.000e+00



Center for Innovation in Ship Design
A Feasibility Study on Numerical Modeling of Large
Scale Naval Fluid Structure: Contact Impact Problems

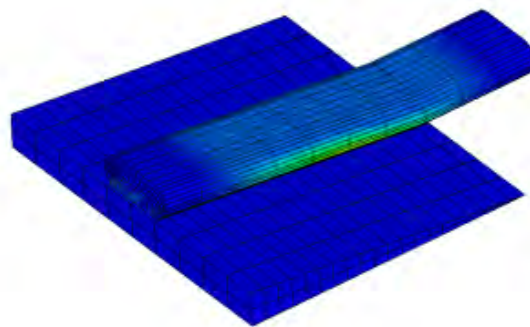
LS-DYNA keyword deck by LS-PrePost
Time = 6.9
Contours of X-stress
max ipt. value
min=-466799, at elem# 35094
max=4.28945e+06, at elem# 34790



Fringe Levels
4.289e+06
3.814e+06
3.338e+06
2.863e+06
2.387e+06
1.911e+06
1.436e+06
9.601e+05
4.845e+05
8.826e+03
-4.668e+05



LS-DYNA keyword deck by LS-PrePost
Time = 12.775
Contours of Effective Stress (v-m)
max ipt. value
min=0, at elem# 28001
max=5.50472e+06, at elem# 34790



Fringe Levels
5.505e+06
4.954e+06
4.404e+06
3.853e+06
3.303e+06
2.752e+06
2.202e+06
1.651e+06
1.101e+06
5.505e+05
0.000e+00



Figure 12 LS-PrePost stress contour plots for a flexible membrane structure (Case-IV)

CONCLUDING REMARKS

The major objective of this study is to assess the feasibility of using an advanced numerical code to simulate the dynamic motion of MOSES under wave action. This is achieved by developing a numerical model of the wave basin with wave generation over a rigid basin bottom to study the dynamic behavior of MOSES under laboratory conditions. The numerical predictions will be compared *qualitatively* with experimental results obtained in an accompanying experimental study by Bloxom *et al* 2010. The simulations thus far utilize an Arbitrary Lagrangian and Eulerian (ALE) technique to capture the multi-physics phenomenon.

Numerical predictions are first used to complement the original experimental data and then the results are used to supplement experimental tests to establish trends for different orientations of the MOSES. The first step in the modeling was to treat MOSES as a fully rigid object and tests its motion under the action of the waves. Results show that the coupled FSI numerical code can successfully capture the motion of MOSES under the severe action of waves.

As a first step the object was placed on top of the movable beach and it was allowed to move freely (at this point of model testing the geometry of the object (MOSES) was not complete owing to the challenge of modeling the membrane structure shape for the object). It was noticed that when the object is left to move freely on the beach, it initially slides on the beach and sinks eventually. This was, however, an important step to comprehend the behavior of each component of the coupled system under the action of the waves in the NWB. The next step in the procedure was to model and attach *springs* at the end of the object to control the motion of the inflatable causeway under the action of waves.

Once the desirable motion of the object is achieved, the subsequent step was to change the stiffness and the weight of the object to obtain a more realistic behavior of the motion. The waves generated in the numerical wave basin were allowed to reflect back after they reach the end of the NWB to observe the motion of the object under the reflective wave.

The numerical test cases were made even more realistic by introducing friction between the beach and the object to capture the physics correctly. Once the spring/weight were successfully modeled and the motion established with an added friction the following simulations were

Center for Innovation in Ship Design

A Feasibility Study on Numerical Modeling of Large
Scale Naval Fluid Structure: Contact Impact Problems

performed under the realistic case of a non-reflecting wave motion replicating a real ocean scenario and the results show accurate physics of the motion of MOSES.

All the test cases described above show good matching of the physics of the wave motion and the motion of the membrane structure on the movable beach and the qualitative behavior compared well with those shown in the experimental test cases. Both the numerical test cases of treating the water-filled membrane (MOSES) as rigid and fully flexible show a realistic behavior of the membrane structure motion under the action of waves. However, the case where the membrane structure was treated as fully flexible was computationally very intensive and it is hard to achieve a number of cycles of the wave motion.

Given the limited time frame available to develop a numerical model and conduct simulation for the inflatable causeway, the present study was carried out using existing computational support available at the time. The computing needed to complete the numerical simulations ranged from 3 hours (with 8 CPUs on the OSU cluster) to 3 days (20 CPUs on a Naval distributed computer cluster). In the future, if and when a robust high performance computing platform is available the numerical analysis of the inflatable causeway can be tested for a fully flexible case of the membrane structure. Specifically, the study can be further extended to the cases of varying orientation of the membrane structure and the movable beach.

REFERENCES

Bloxom, A., Medeling, A., Vince, C and Yim, C.S., 2010. "Modeling and testing of inflatable structures for rapidly deployable port infrastructures," *Technical report NSWCCD-CISD-2010/010-Ship System Integration and Design Department*, Naval Surface Warfare Center, Carderock Division, West Bethesda, MD 20817-5700.

Belytschko, T., Flanagan, D. F., and Kennedy, J. M., 1982. "Finite element method with user-controlled meshes for fluid-structure interactions," *Computer Methods in Applied Mechanics and Engineering*, **33**, pp. 689–723.

Dickens, K., and Rosen, P., 2007. "MOSES-Inflatable Causeway" *Technical report NSWCCD-CISD-2007/005-Ship System Integration and Design Department*, Naval Surface Warfare Center, Carderock Division, West Bethesda, MD 20817-5700.

Hallquist, J. O., 2006. "LS-DYNA Theory Manual," *Livermore Software Technology Corporation*.

Tokura, S., and Tetsuli, I., 2005. "Simulation of wave dissipation mechanism on submerged structure using fluid-structure coupling capability in LS-DYNA", *5th European LS-DYNA users conference*, pp. 2c-37.

Souli, M., Olovsson, L., and Do, I., 2002. "ALE and fluid-structure interaction capabilities in LS-DYNA," *7th International Users Conference*, May 19-21, Dearborn, Michigan, USA.

APPENDIX

LS-DYNA SPECIFIC MODELING PROCEDURE

In this appendix, details of the numerical simulation procedure specific to modeling the physical wave basin and water-filled membrane (MOSES) using a multi-physics multi-scale finite-element code LS-DYNA are delineated. Specifically, a nine-step simulation procedure pertaining to such class of fluid-structure interaction problems are shown.

STEP 1: Modeling Wave Basin and Various Components

The wave basin consists of the following domains:

- 1) Water Domain
- 2) Air Domain
- 3) Wavemaker
- 4) Movable Beach
- 5) Membrane Structure
- 6) Springs

Creating Objects in LS-DYNA

Dimensions of Water and Air Domain of Numerical Wave Basin (NWB):

The original length of the water domain is 13.8m (45.5 ft) and the width of the water domain is 5.6m (18.5 ft). The height of the water column is 0.254m (10 in). Figure 9 shows the elevation of the water domain in 2-D. The length of the water domain has been discretized into 139 Elements (with an element size of 0.1m). The wavemaker was located 2m (82in) from the left end of the wave basin. The height of the wavemaker is 0.7112m (28in) and its width is that of the wave basin. Isometric view of the numerical wave basin is shown in Figure10.

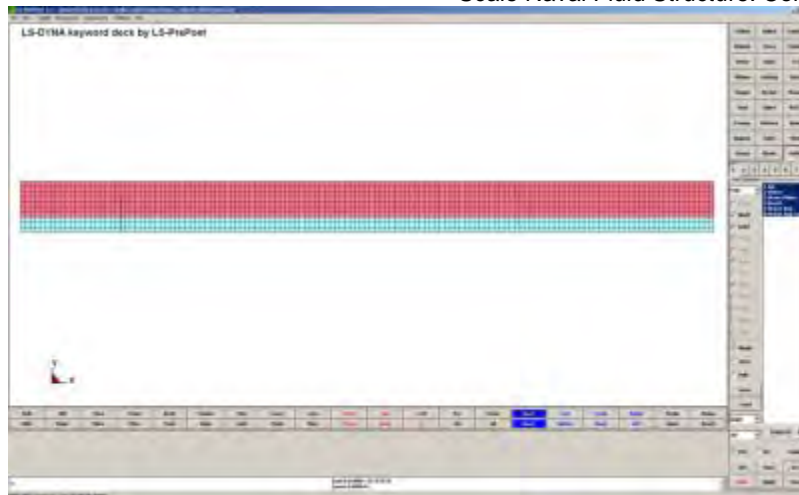


Figure 13 Elevation of Waver-Air domain of actual wave basin
(Green: Water domain and Red: Air domain)

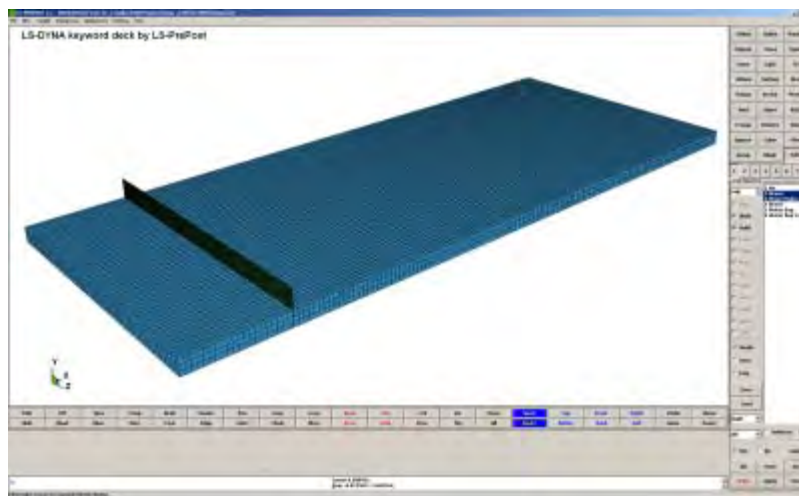


Figure 14 Isometric view of actual wave basin

Numerical Model of Wave Basin:

In the physical experiment, there was material present at the back of the wave basin to provide energy absorption to prevent wave reflection. The physical nature of the material is not important and the absorption effect can be modeled numerically using an absorbing boundary condition. The run time of the numerical model can be significantly reduced without sacrificing accuracy in capturing the physics of the wave motion and the motion of the membrane structure by placing

the absorbing boundary sufficiently farther downstream of the structure. In this study, a water domain length of 4.98m (16.3ft) is deemed sufficient. Water and air domain has been created with solid elements. Elevation of the water domain is shown in Figure 11.

Eight-node brick elements and four-node Belytschko-Tsey shell elements have been used for discretization of the NWB. Solid brick elements are used for air/water/movable beach domains and shell elements for membrane structure/wavemaker domains.

Part 1: Water Domain:

The dimensions of the wave basin are as follows:

Length of the water domain = 4.98m (16.3ft)

Width of the water domain= 5.6m (18.5 ft)

Height of the water domain= 0.254m (10 in)

Size of the element=0.1m (so the no. of elements per length is 50)

The elevation of the water domain is shown in Figure 11.

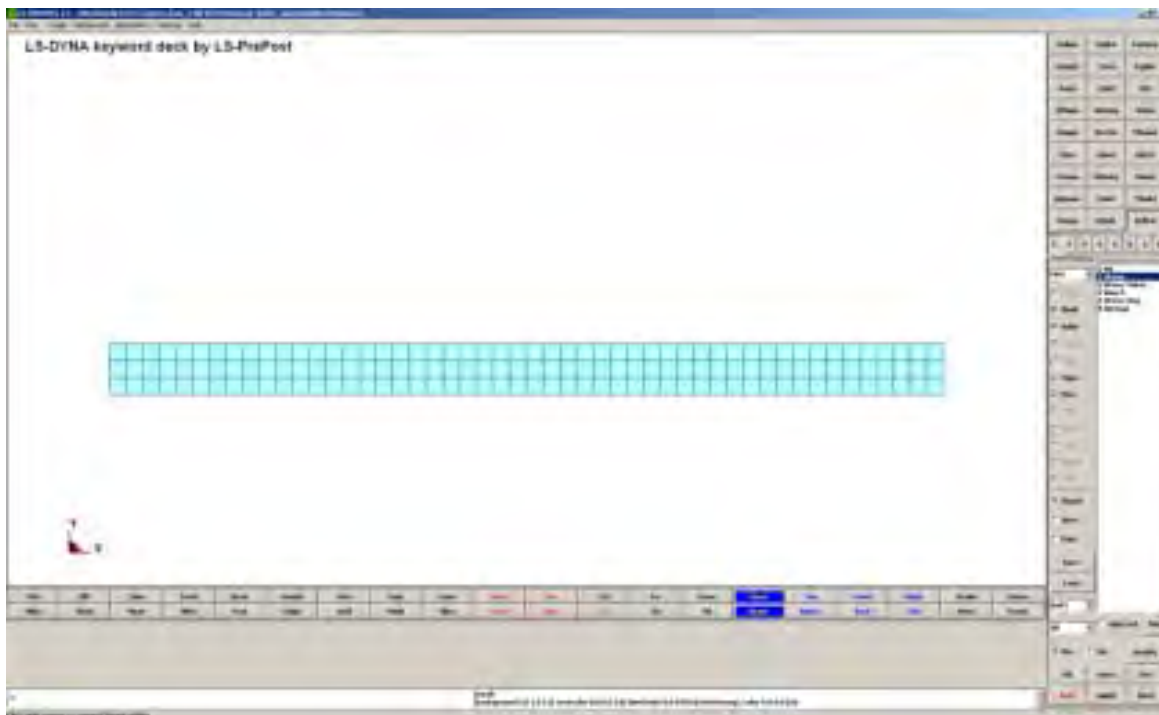


Figure 15 Elevation of water domain (2D-view)

Part 2: Air Domain

The dimensions of the air domain are as follows:

Length of the air domain = 4.98m (16.3ft)

Width of the air domain = 5.6m (18.5 ft)

Height of the air domain = 0.72m (30in)

Size of the element = 0.1m (so the no. of elements per length is 50)

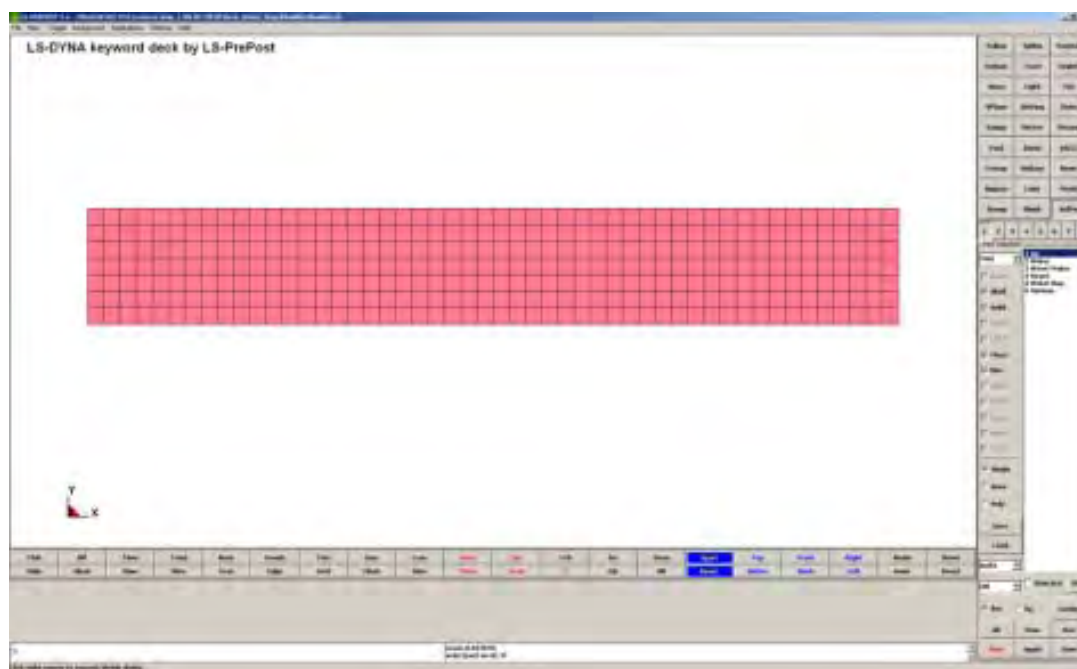


Figure 16 Elevation of air domain (2D-view)

Note: In order to visualize/capture the free surface in LS-DYNA an air domain on top of the water domain is required. A criteria to choose the height of the air domain is based on the maximum wave height (usually the height of the air domain is chosen in such a way that it is larger than the maximum wave height). Figure 12 shows the elevation of the air domain in 2-D and Figure 13 shows the elevation of both the air and water domain in the numerical wave basin.

Visualization of Water and Air domain

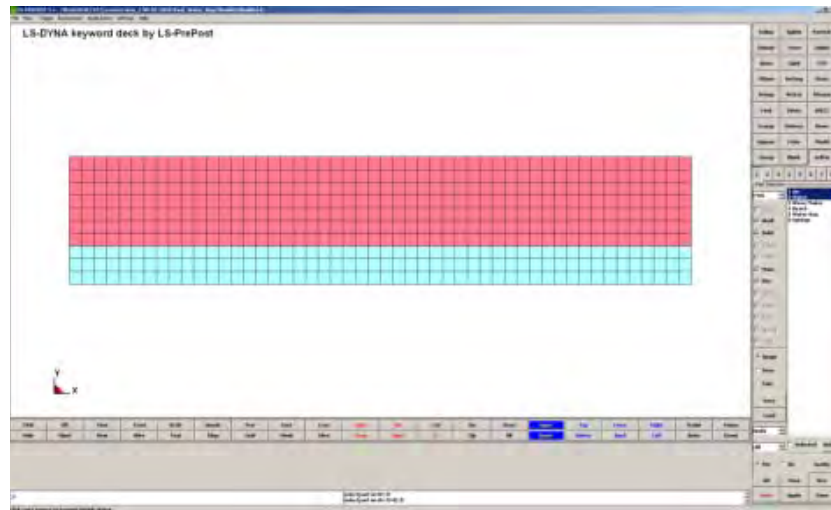


Figure 17 Elevation of air and water domain (2D-view)

Figures 14 and 15 show three dimensional views of the water and air domains. Figure 15 shows a transparent view of the air and water domain. This feature is a key in visualizing the wave motion and the movement of the membrane structure once the wavemaker starts moving. It can also be used to plot the velocity vectors across the domain.

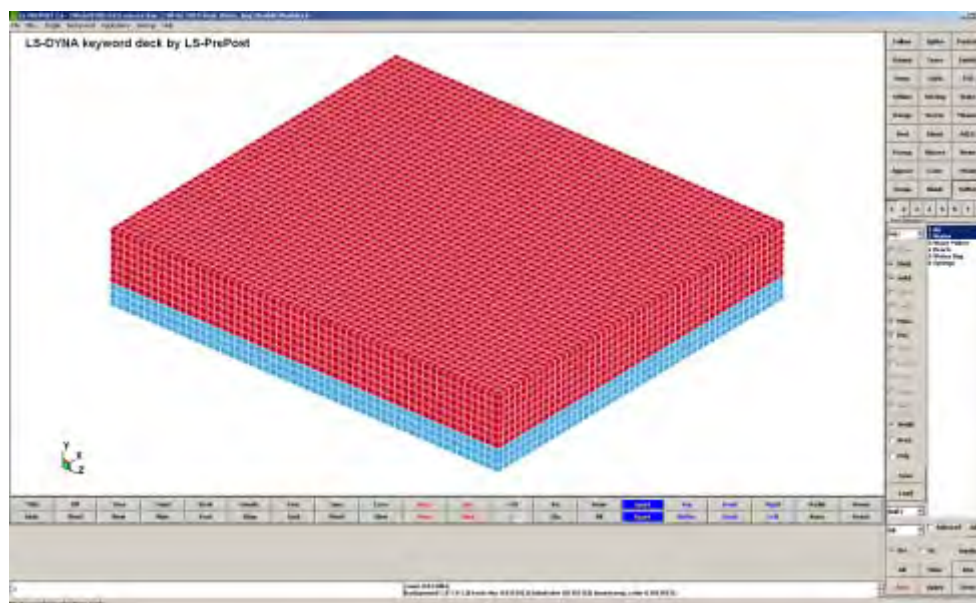


Figure 18 Isometric view of air and water domains (3D)

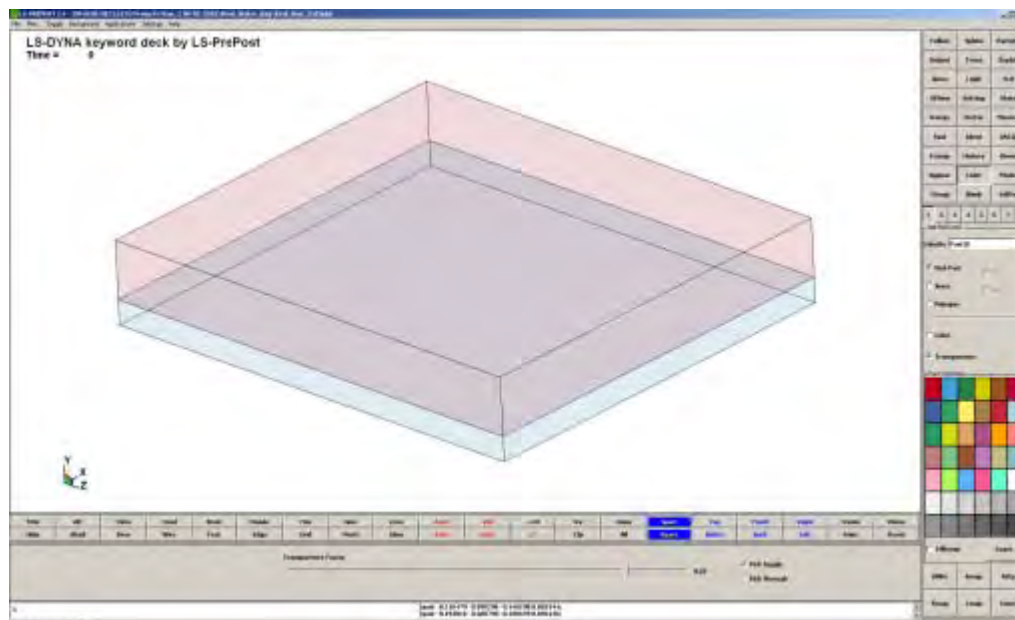


Figure 19 Transparent view of air and water domains

Part 3: Wavemaker

A piston-type wavemaker is used to generate prescribed regular waves or irregular waves from specific spectra. The wavemaker has a 6" maximum stroke and the frequency of the waves has a 2 Hz maximum. For the current simulation a stroke of 3" with a maximum frequency of 1Hz is used. The wavemaker is made of shell elements (Figure 16). The Belytschko-Tsay formulation (Hallquist, 2006) is used for the shells and the thickness of the shell is 0.05m. The most important part is the orientation of the normals of the wavemaker. Specifically, the normals have to be in the direction of the wave generation (Figure 17). The height of the wavemaker is 0.7112m (28in) and the model width is that of the physical wave basin.

Center for Innovation in Ship Design
A Feasibility Study on Numerical Modeling of Large
Scale Naval Fluid Structure: Contact Impact Problems

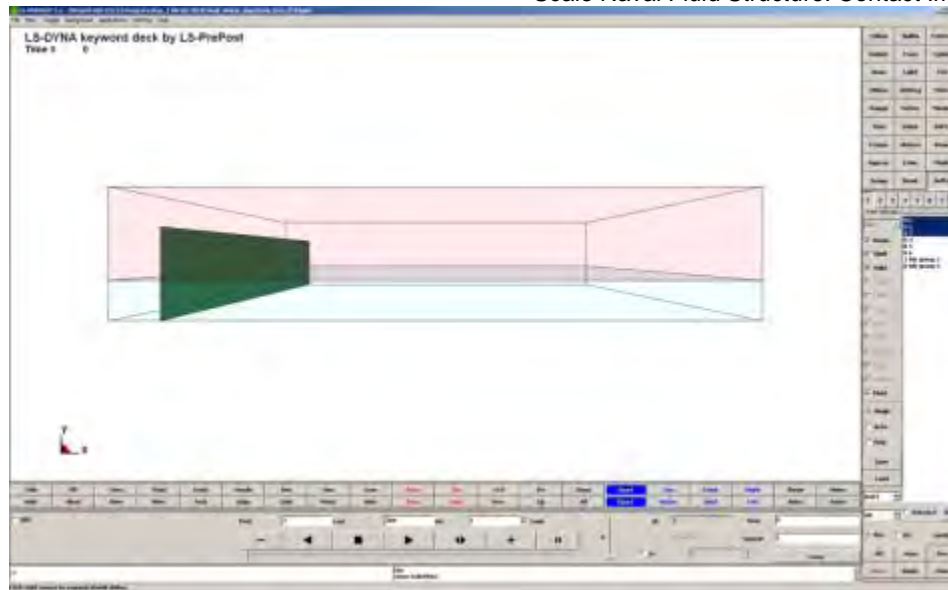


Figure 20 Isometric view of face of wavemaker and front view of water domain

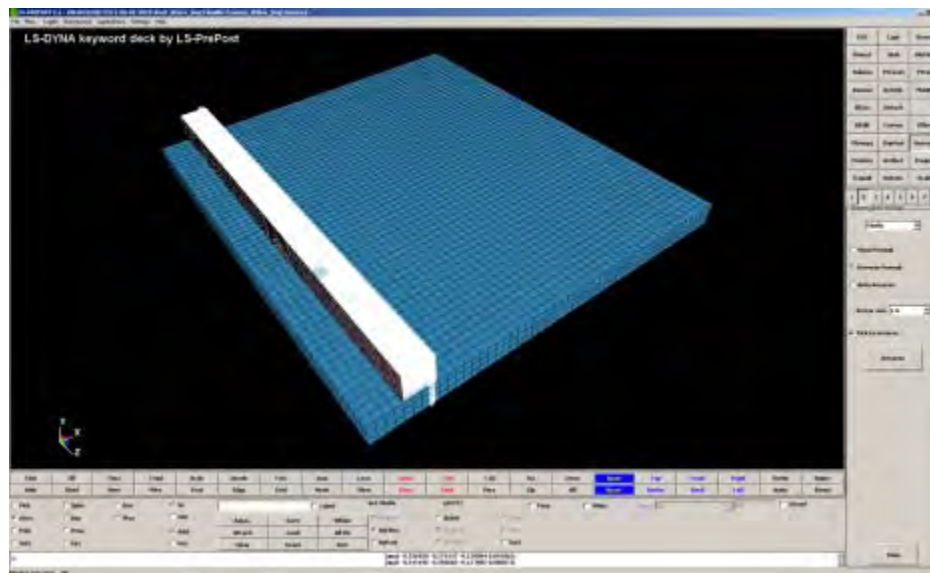


Figure 21 Vector normals of wavemaker in line with water domain

Part 4: Movable beach

The movable beach is made of solid elements (Figure 18) and has the following dimensions:

Height=0.24m (9.75")

Width =2.4m (96")

Length =2.08m (82")

Slope=1:8.4

In this preliminary study, the beach is modeled as fixed to capture the physics of the motion of the membrane structure correctly.

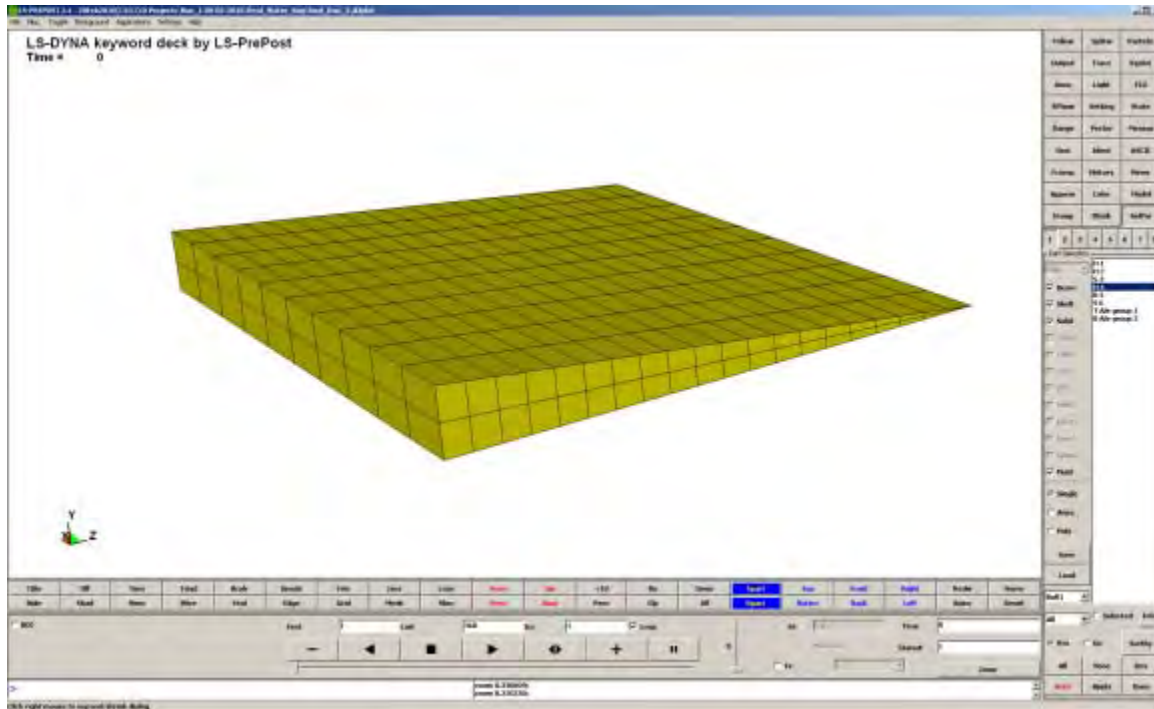


Figure 22 Movable Beach

Part 5: Membrane Structure

The membrane structure, made up of shell elements, is placed on top of the movable beach. Modeling of the membrane structure is one of the most challenging parts of the current study (in addition to achieving the correct physics). The dimensions of the membrane structure are 3.048m (10ft) in length, 0.2286m (0.75ft) in width, and 0.2286m (0.75ft) in height, respectively. Figure 19 shows the membrane structure on top of the beach.

Center for Innovation in Ship Design
A Feasibility Study on Numerical Modeling of Large
Scale Naval Fluid Structure: Contact Impact Problems

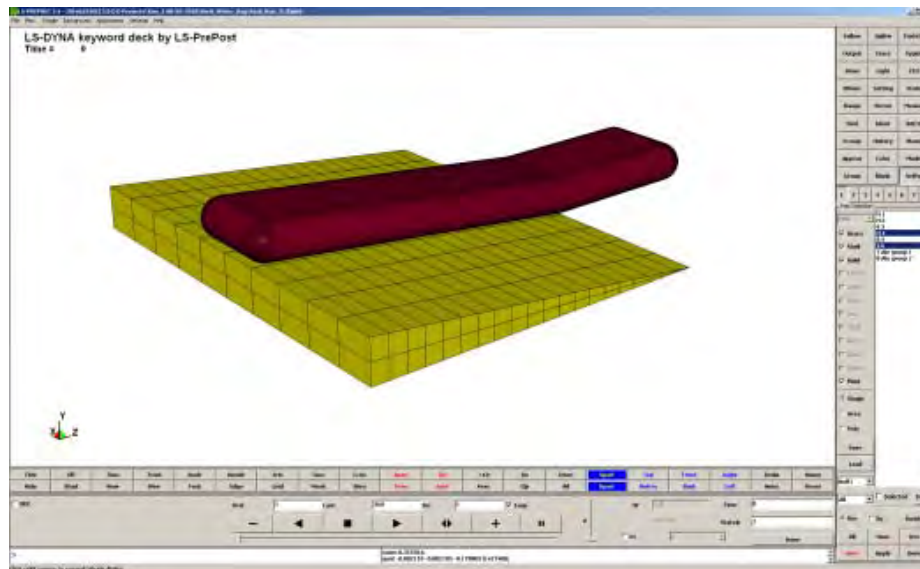


Figure 23 Membrane structure and movable beach

After all the five parts have been modeled independently they are then assembled to get the components ready for numerical simulation. Figure 20 shows the assembly of air and water domain, wavemaker, solid wedge (movable beach) and the membrane structure. Figure 20 shows the side view of the assembly. An isometric view of the complete assembly is shown in Figure 21.

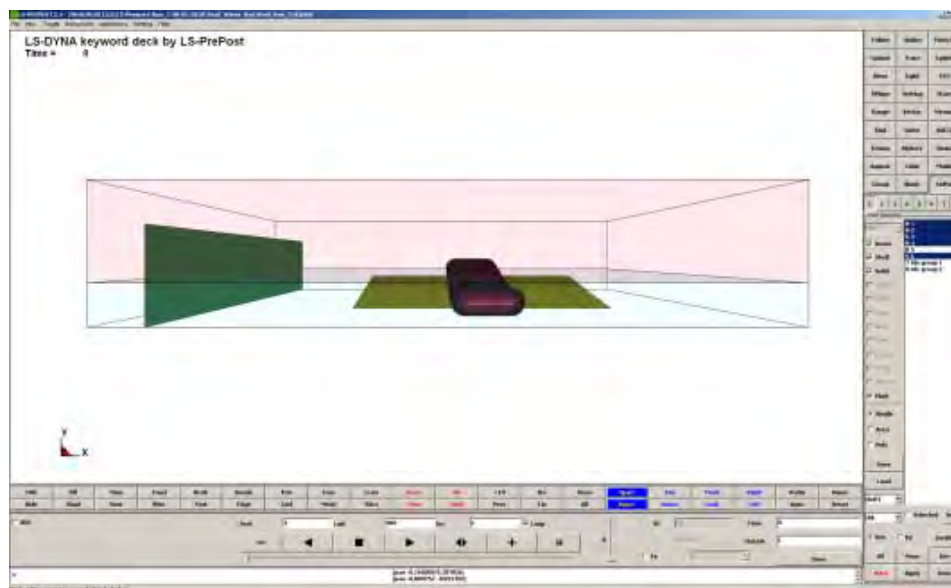


Figure 24 Complete assembly of air, water, wavemaker, beach and membrane structure

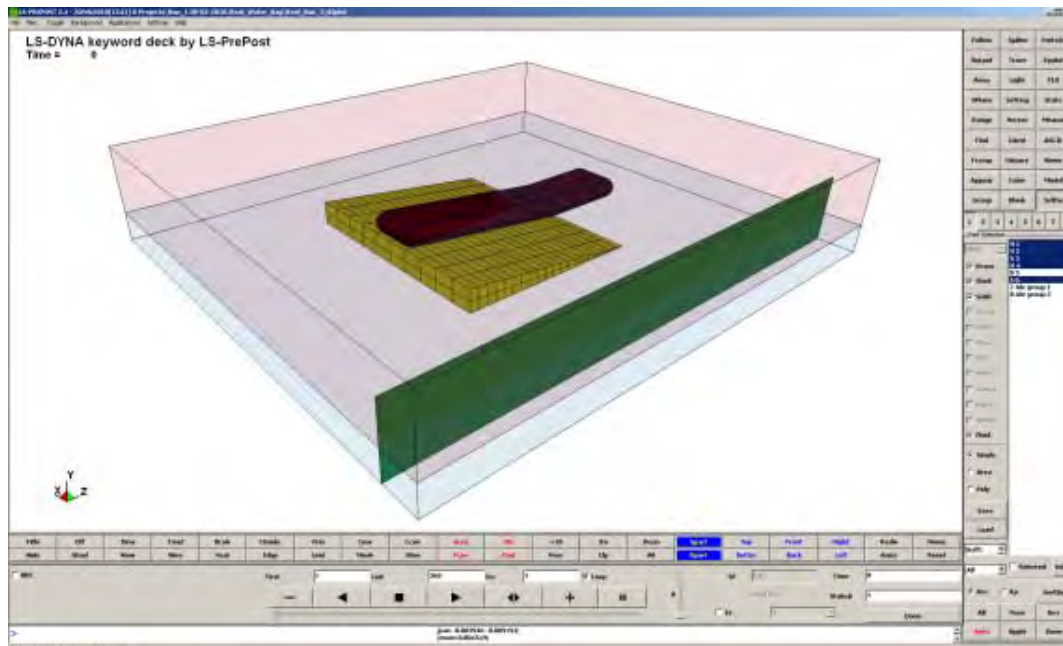


Figure 25 Up-close of complete assembly (view from the wavemaker side)

Part 6: Constraint Spring Modeling

Two springs were attached to the membrane structure to restrain one end. The idea of modeling springs is essential in the current simulation as without them the membrane structure would slide freely on the moveable beach and move with the wave which is not desirable and practical. With the springs, one end of the membrane structure is restrained. However, the membrane structure is free to rotate about the z-axis along the restrained end.

Modeling Technique:

The springs have been modeled using discrete elements (by picking four duplicate end nodes of the membrane structure). These nodes become the basis for the formation of the spring elements and they have been assigned a mass value of 10kg each. Once the springs are modeled, the next step is to detach two nodes and extend them in the z-direction to set the spring form. The remaining two free nodes of the spring are then merged with the membrane structure. The spring constant (K) of 10,000N/m seem to hold the membrane structure in place (a trial-and-error approach was used in determining the spring constants). Figure 22 shows an up close view of the springs and the membrane structure. It is important to note that the springs are treated as fully

Center for Innovation in Ship Design
A Feasibility Study on Numerical Modeling of Large
Scale Naval Fluid Structure: Contact Impact Problems

flexible to allow them to move freely with the motion of the bag. A isometric view of the movable beach with the springs attached to the membrane structure is shown in Figure 23.

As a part of the membrane structure rests on the bottom of the water basin friction has to be defined between the membrane structure and the water basin and it has to be defined along with the springs attached to the end of the membrane.

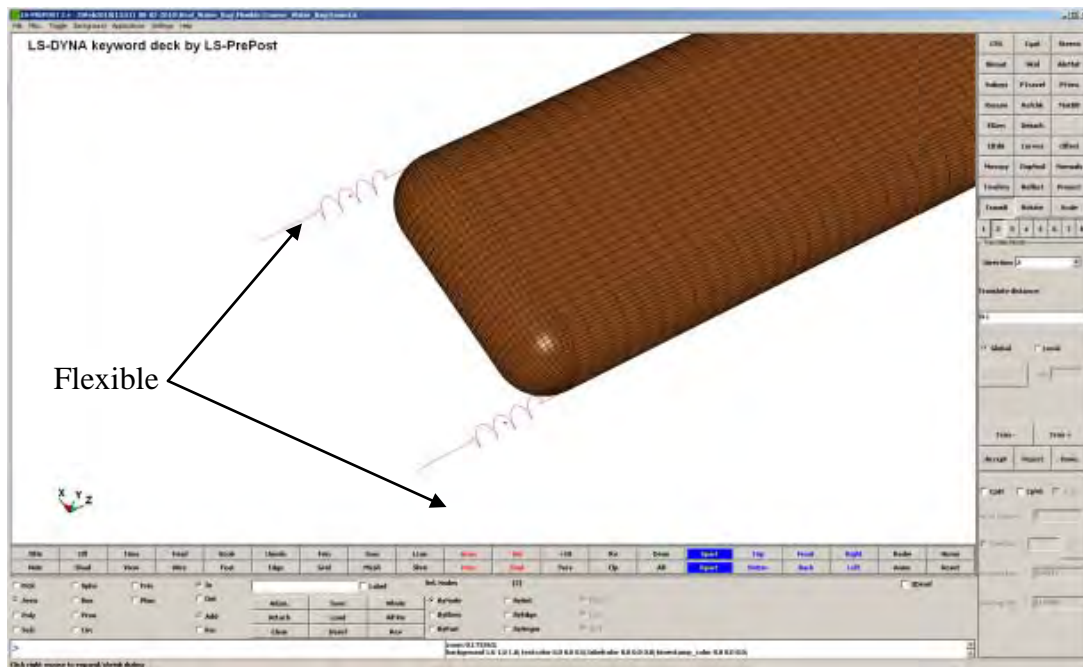


Figure 26 Up-close of springs attached to membrane structure

Center for Innovation in Ship Design
A Feasibility Study on Numerical Modeling of Large
Scale Naval Fluid Structure: Contact Impact Problems

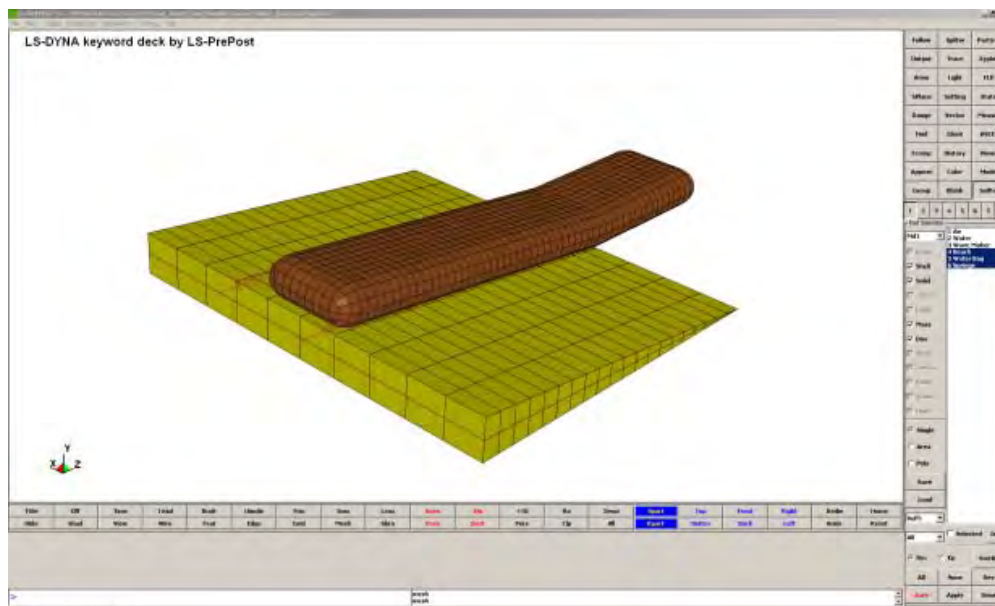


Figure 27 Isometric view of movable beach and springs attached to membrane structure

Finally, a snapshot of the complete model information with the total number of nodes, elements and materials is shown in Figure 24.

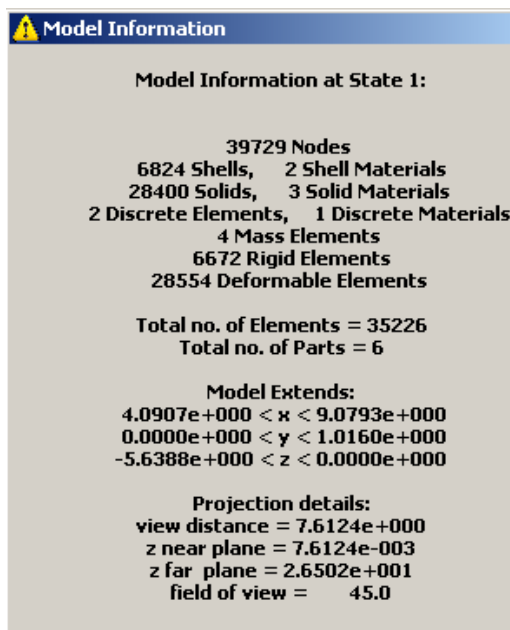


Figure 28 Complete model information for simulation of numerical wave basin

STEP 2: Material Models

Part 1: Water Domain

As recommended by the LS-DYNA theory manual, to model fluid domain “Material_Null” is used. For solid elements the “Material Null” is the material model that has to be used to invoke the equations of state (EOS) to avoid deviatoric stress calculations. (Hallquist, 2006). The Null material model demands the use of Gruniesen equation of state for a complete definition of fluid contact modeling. The properties of water that are needed for this card are as follows:

Density = 1000 kg/m³

Pressure cut-off = -1.0E+26 N/m²

Viscosity = 1.0E-03 N*s/m²

As mentioned above the water domain needs an equation of state to capture the fluid behavior (which is implemented by defining an EOS card). In physics and thermodynamics, an EOS is a relation between state variables. It is a constitutive equation which provides a mathematical relationship between two or more state functions associated with the matter, such as its temperature, pressure, volume, or internal energy. Equations of state are useful in describing the properties of fluids, mixtures of fluids, solids, and even the interior of stars.

Detailed description of the equation of state for water (the Gruniesen equation) is described as follows.

The Gruniesen equation of state with cubic shock velocity-particle velocity defines pressure for compressible material is governed by

$$P = \frac{\rho_0 C^2 \mu \left[1 + \left(1 - \frac{\gamma_0}{2} \right) \mu - \frac{a}{2} \mu^2 \right]}{\left[1 - (S_1 - 1) \mu - S_2 \frac{\mu^2}{\mu + 1} - S_3 \frac{\mu^3}{(\mu + 1)^2} \right]} + (\gamma_0 + \alpha \mu) E \quad (1)$$

where E is the internal energy per initial volume, C (speed of sound) is the intercept of the shock velocity-particle velocity curve (Us-Up), S_1 , S_2 and S_3 are the coefficients of the slope of the us-up curve, γ_0 is the Gruniesen gamma, and a is the first order volume correction to γ_0 . The constants C , S_1 , S_2 , S_3 , γ_0 , and a are all input parameters. Compression is defined in terms of the relative volume, V , as: $\mu = \frac{1}{V} - 1$. For expanded materials, the pressure is defined by:

$P = \rho_0 C^2 \mu + (\gamma_0 + \alpha \mu) E$. ρ_0 is the reference density. The input used in the Gruniesen equation is given in Table 1 (Hallquist, 2006).

Table 1: Gruniesen Parameters for Water

Equation of State (Parameter)	Card value (from manual)
C	100 m/s
S_1	1.979
S_2	0.0
S_3	0.0
γ_0	0.11
A	0.0
E_0	0.0
V_0	0.0

Part 2: Air Domain

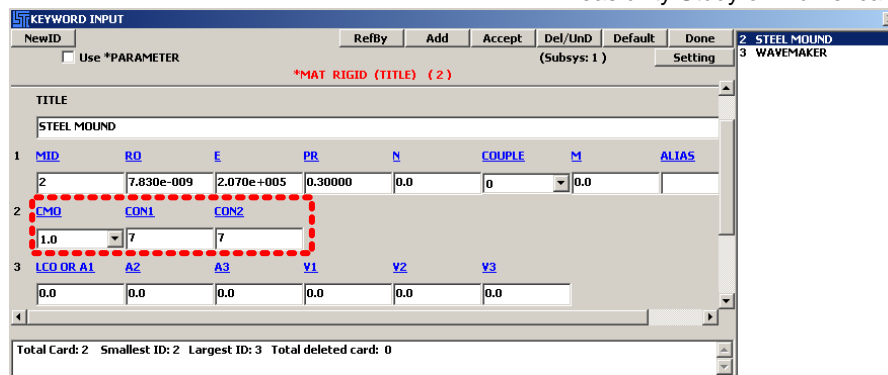
Material_Vacuum is used for the air domain. The only parameter this card demands is the density of air and the value is set to zero.

Part 3: Wavemaker

The wavemaker is treated as rigid. Hence, Material_Rigid is used for this purpose. The properties of steel are generally used and Figure 25 shows the value inputs for this card. It is important to mention that CMO, CON1 and CON2 are the values which assign constraints on the global motion of the wavemaker. The values of 1, 5 and 7 specify that the motion of the wavemaker is only in the positive x-direction interacting with the fluid.

Note:

- Use “CMO” (Center of Mass Constraint Option) to set BC’s of both the mound and wavemaker
- “CON1” = Translational constraint
- “CON2” = Rotational constraint
- The wavemaker uses “5” and “7” (allows it to move in only X-translational direction)



	MID	RO	E	PR	N	COUPLE	M	ALIAS
1	2	7.830e-009	2.070e+005	0.30000	0.0	0	0.0	
2	CMO	CON1	CON2	1.0	7	7		
3	LCO OR A1	A2	A3	V1	V2	V3	0.0	0.0
4								

Total Card: 2 Smallest ID: 2 Largest ID: 3 Total deleted card: 0

Figure 29 Material properties for wavemaker

Part 4: Movable Beach

The movable beach is made up of solid elements and it is treated as rigid. Hence, just like the wavemaker the beach uses the Material_Rigid with the same properties as of the wavemaker. The only major difference however is that the beach is fixed globally so the values of CMO, CON1 and CON2 are 1, 7 and 7, respectively.

Part 5: Membrane Structure

The membrane structure too is treated as rigid. So Material_Rigid is used with CMO, CON1 and CON2 as 1, 0 and 0 respectively as the membrane structure is free to move. The properties of steel used for the wavemaker and movable beach are retained.

Part 6: Springs

The springs are modeled first as rigid and then as a flexible part. For rigid case as mentioned above Material_Rigid is used with the properties of steel and when it is treated as a flexible part Material_Spring_Elastic is used. Figure 26 shows the card values for the elastic case.



	MID	K
6	1.000e+004	

6 Springs

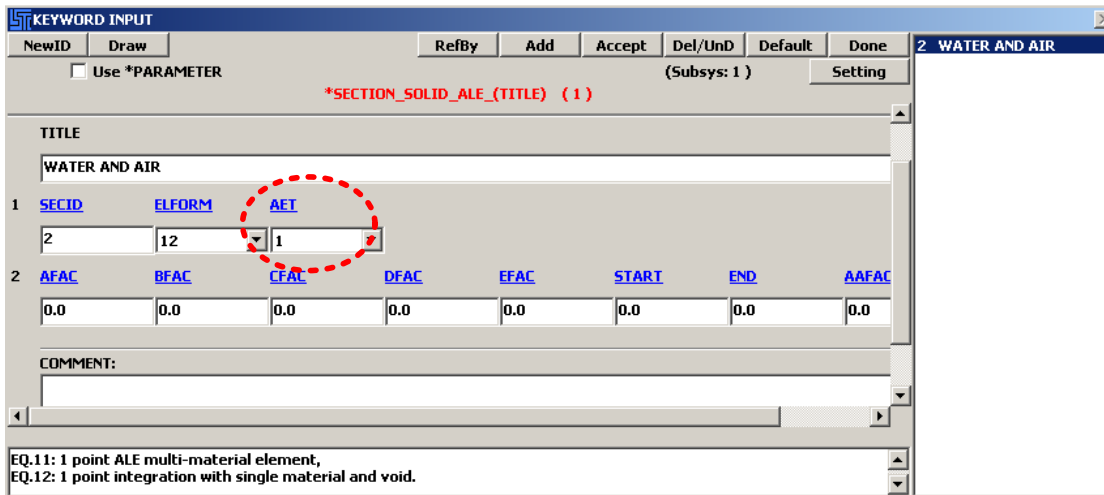
Figure 30 Material properties for springs

STEP 3: Element/Section Properties

Eight-node brick elements and four-node Belytschko-Tsey shell elements have been used for discretization of the NWB. Solid brick elements are used for air/water/movable beach domains and shell elements for membrane structure/wavemaker domains. The Belytschko-Lin-Tsey shell element is implemented in LS-DYNA as a computationally efficient alternative to the Hughes-Liu shell element (Hallquist, 2006) used earlier. For a shell element with five through-the-thickness integration points, the Belytschko-Lin-Tsey shell elements requires 725 mathematical operations compared to 4066 operations for the under-integrated Huges-Liu shell elements. Because of its computational efficiency, the Belytschko-Lin-Tsey shell element is usually the shell element formulation of choice. The Belytschko-Lin-Tsey shell element is based on a combined co-rotational and velocity-strain formulation. The efficiency of the element is obtained from the mathematical simplifications that result from these two kinematical assumptions. The co-rotational portion of formulation avoids the complexities of non-linear mechanics by embedding a coordinate system in the element. The choice of velocity-strain rate of deformation in the formulation facilitates the constitutive evaluation, since the conjugate stress is the more familiar Cauchy stress. Detailed formulation of this element is given in LS-DYNA theory and keyword manual.

Part 1: Water Domain

The water domain is modeled using an ALE formulation which forms the basis for all FSI problems. Figure 27 shows the card details for Solid_ALE.



KEYWORD INPUT

NewID Draw RefBy Add Accept Del/UnD Default Done 2 WATER AND AIR

☐ Use *PARAMETER (Subsys: 1) Setting

*SECTION_SOLID_ALE_(TITLE) (1)

TITLE

WATER AND AIR

	SECID	ELFORM	AET	AFAC	BFAC	CFAC	DFAC	EFAC	START	END	AAFAC
1	2	12	1								
2				0.0	0.0	0.0	0.0	0.0	0.0	0.0	0.0

COMMENT:

EQ.11: 1 point ALE multi-material element,
EQ.12: 1 point integration with single material and void.

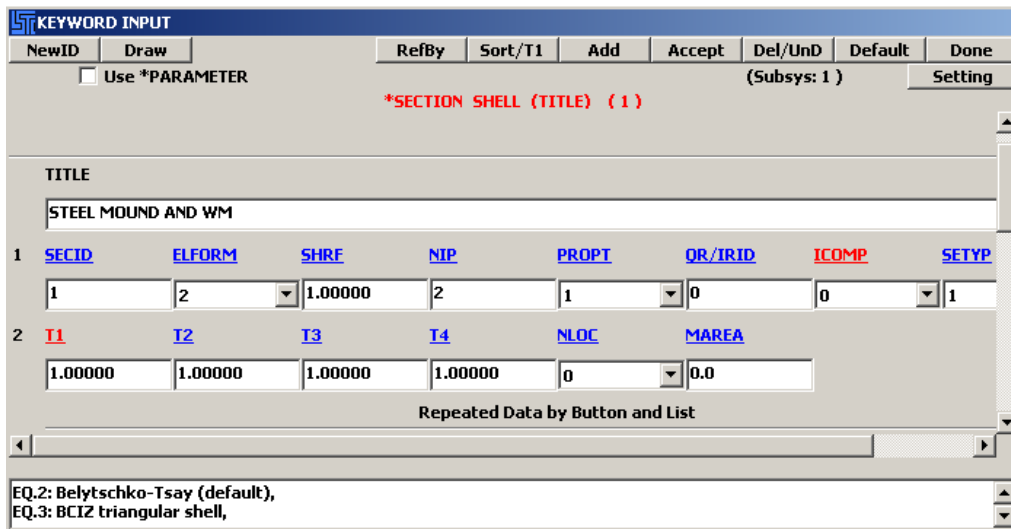
Figure 31 Section properties for water domain

Part 2: Air Domain

The air domain is also modeled using Solid_ALE. The card values as shown in Figure 25 are retained for the air domain. However, the air domain does not need an equation of state.

Part 3: Wavemaker

The wavemaker is modeled using shell elements. Figure 28 shows the card values for Section_Shell. Belytschko_Tsay element formulation (ELFORM-2) is used for this purpose and the thickness of the shell is chosen as 0.05m.



The screenshot shows the 'KEYWORD INPUT' dialog box for a 'SECTION SHELL (TITLE) (1)'. The 'TITLE' field is set to 'STEEL MOUND AND WM'. The 'Use *PARAMETER' checkbox is unchecked. The 'Subsys: 1' is selected. The 'Setting' button is visible. The 'EQ.2' field is set to 'Belytschko-Tsay (default)', and the 'EQ.3' field is set to 'BCIZ triangular shell'.

RefBy	Sort/T1	Add	Accept	Del/UnD	Default	Done
1	2	1.00000	2	1	0	0
2	1	1.00000	1.00000	1.00000	1.00000	0

Repeated Data by Button and List

EQ.2: Belytschko-Tsay (default),
EQ.3: BCIZ triangular shell,

Figure 32 Section properties for wavemaker

Part 4: Movable Beach

The beach is modeled using regular solid elements. The following are some of the options that are available for the solid element (Hallquist, 2006). Figure 29 shows the section properties for the beach.

ELFORM: Element formulation options

EQ.0: 1 point corotational for *MAT_MODIFIED_HONEYCOMB

EQ.1: constant stress solid element (default)

EQ.2: fully integrated S/R solid

EQ.3: fully integrated quadratic 8 node element with nodal rotations

- EQ.4: S/R quadratic tetrahedron element with nodal rotations
EQ.5: 1 point ALE
EQ.6: 1 point Eulerian
EQ.7: 1 point Eulerian ambient, EQ.8: acoustic
EQ.9: 1 point corotational for *MAT_MODIFIED_HONEYCOMB
EQ.10: 1 point tetrahedron etc.
EQ. 1 i.e., the Constant Stress Solid Element is used in the present case.

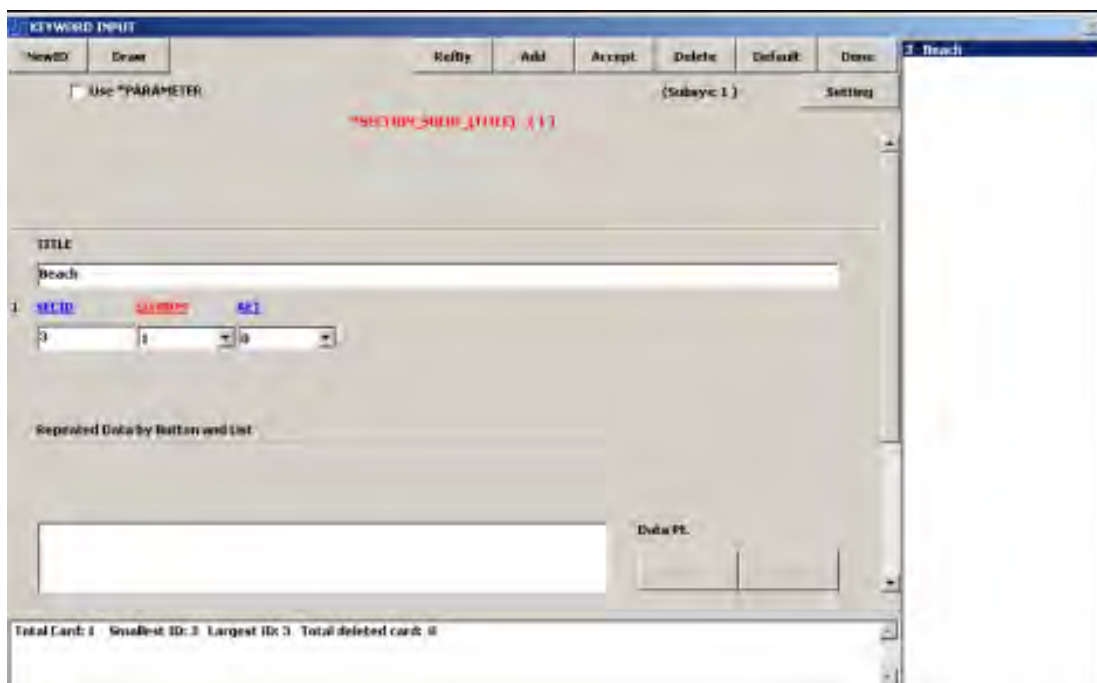


Figure 33 Section properties for movable beach

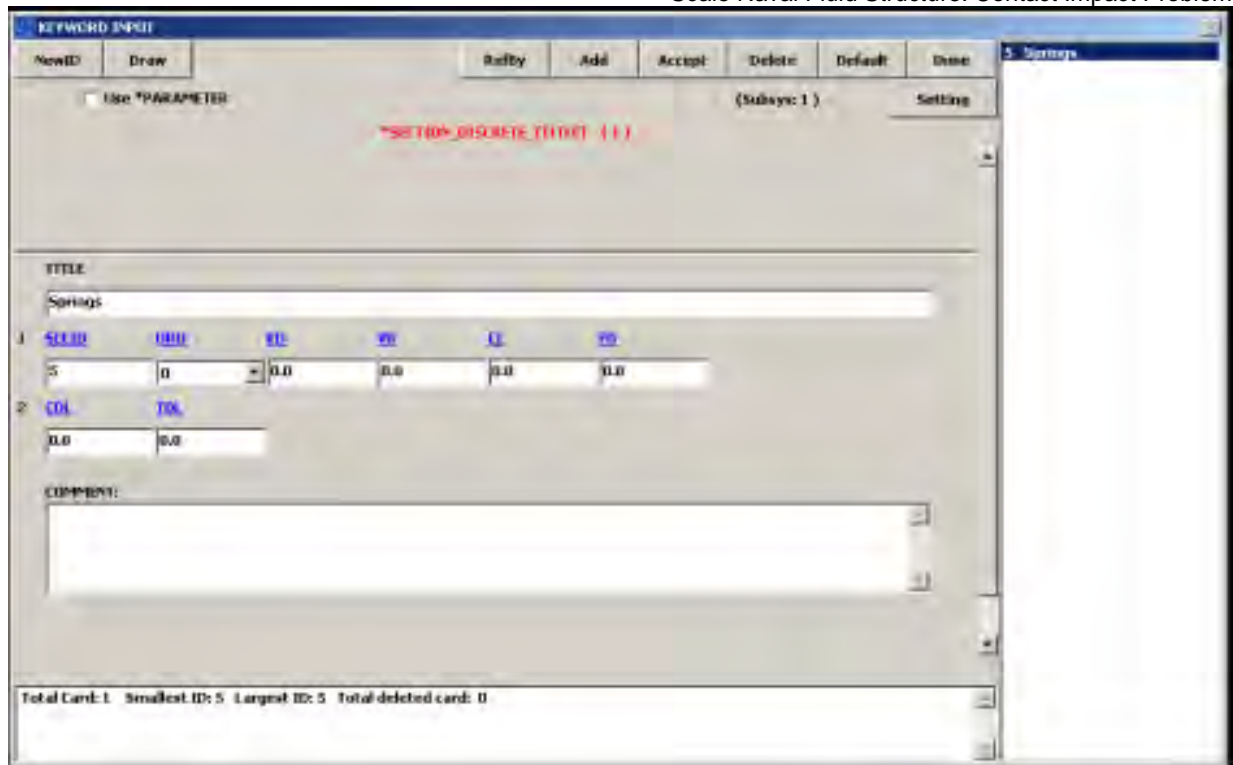
Part 5: Membrane Structure

The membrane structure is modeled using shell elements and the same formulation as used for the wavemaker is used. The membrane weight in the present study is negligible compared to the weight of water.

Part 6: Springs

Springs are modeled using discrete elements. Figure 30 shows the card details for the discrete elements. The default of zero are used for all the card values.

Center for Innovation in Ship Design
A Feasibility Study on Numerical Modeling of Large
Scale Naval Fluid Structure: Contact Impact Problems



KEYWORD INPUT

NewID Draw RefBy Add Accept Delete Default Done 5 Springs

☐ Use *PARAMETER (Subsys: 1) Setting

SETID DISCRETE THICKET ()

TITLE
Springs

ID	TYPE	STIFF	STIFF	STIFF	STIFF	STIFF
5	0	0.0	0.0	0.0	0.0	0.0
7	0.0	0.0				

COMMENT:

Total Card: 1 Smallest ID: 5 Largest ID: 5 Total deleted card: 0

Figure 34 Section properties for defining spring elements

STEP 4: Assigning Material and Section properties

Figure 31 shows the way to assign the various material and section properties to various components. This forms a very important part of the modeling as a proper way of assigning these cards can lead to error free runs.

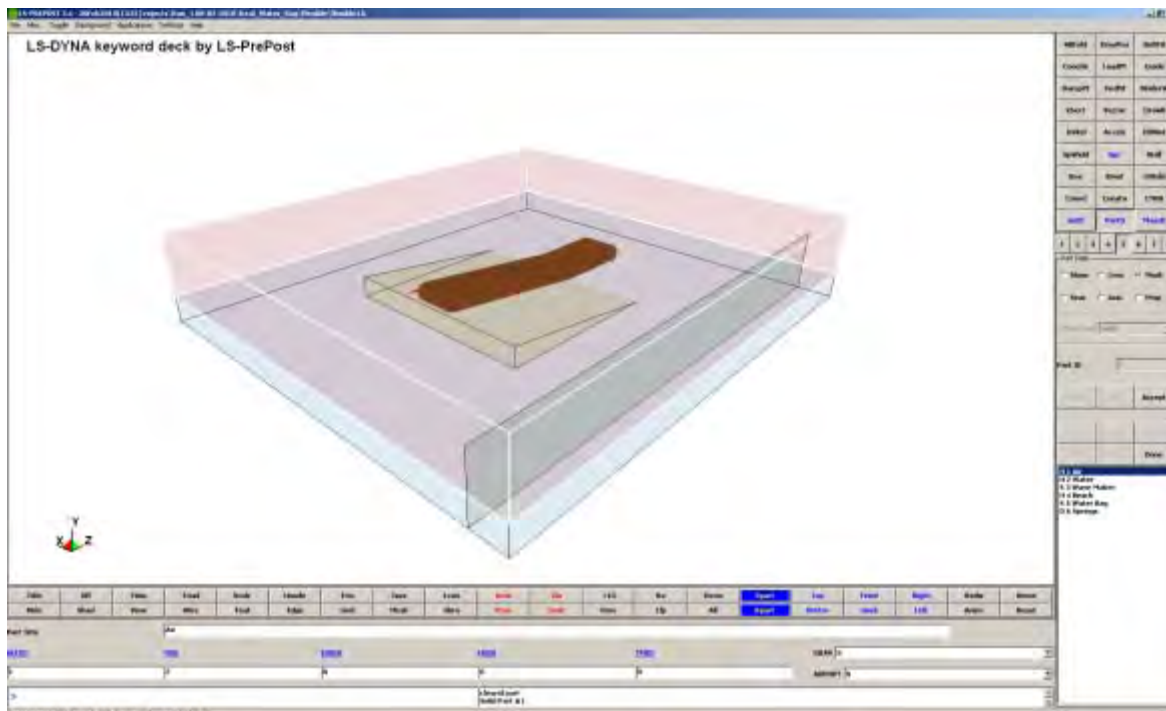


Figure 35 Assigning material/section/EOS data to all the parts in LS-PREPOST

STEP 5: Boundary Conditions

The boundary conditions of the numerical model can be specified by using *Set_Nodes. To define the boundary conditions for the fluid domain in a convenient way, the *Set_Node option is used to combine nodes that have the same BC's. First highlight only those parts to which the modeler wants to create a node set. Figure 32 shows the boundary conditions defined for wave basin. The figure highlights the constraints applied to the nodes on the wall of the wave basin only.

```
1 - Fix_XYZ (nodenum=8)(sub:1)
2 - Fix_XY (nodenum=220)(sub:1)
3 - Fix_XZ (nodenum=36)(sub:1)
4 - Fix_YZ (nodenum=196)(sub:1)
5 - Fix_X (nodenum=495)(sub:1)
6 - Fix_Y (nodenum=5390)(sub:1)
7 - Fix_Z (nodenum=882)(sub:1)
8 - Fix_XYZ_Spring (nodenum=2)
```

These are the eight node sets created to define the constraints on the nodes at various locations in the wave basin

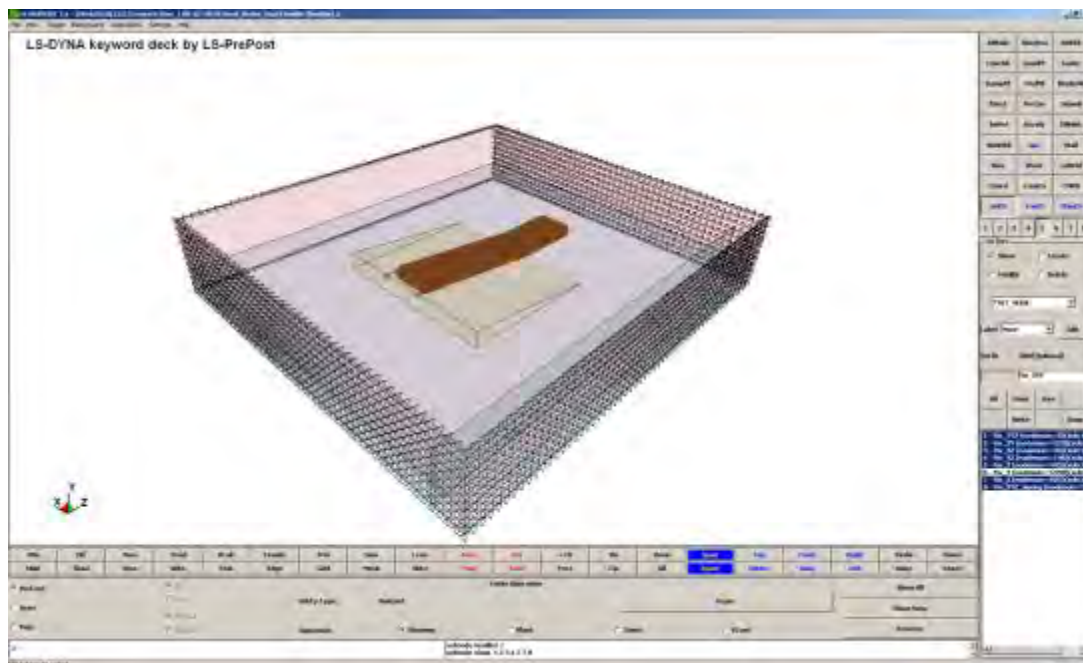


Figure 36 Application of boundary conditions

Boundary_SPC_Set Definitions

Once the node sets have been created using the node set option, the next step is to assign these nodes to the Boundary_SPC_Set card to complete the process of defining various constraints of motion on the nodes of the wave basin. Figure 33 shows the SPC set card. In the figure, the Fix_XYZ node constraints are shown.



Figure 37 Boundary SPC set card definition

Non-Reflecting Boundary Condition Definition

The end of the wave basin where there is no wavemaker, the boundary is specified as non-reflecting. In order to define the non-reflection boundary condition, the first and foremost task is to create a segment set for the non-reflective side. Figure 34 shows the segment sets that have been created. Figure 35 shows the card where the non-reflection BC is defined.

Center for Innovation in Ship Design
A Feasibility Study on Numerical Modeling of Large
Scale Naval Fluid Structure: Contact Impact Problems

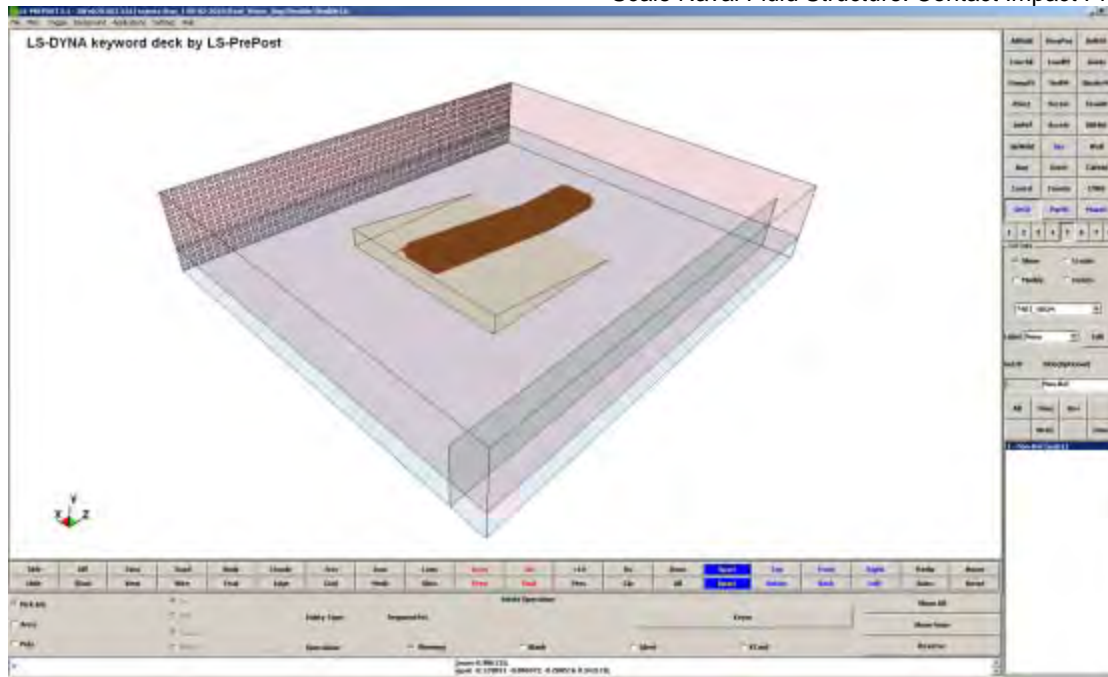


Figure 38 Segment set created to define the non-reflecting BC

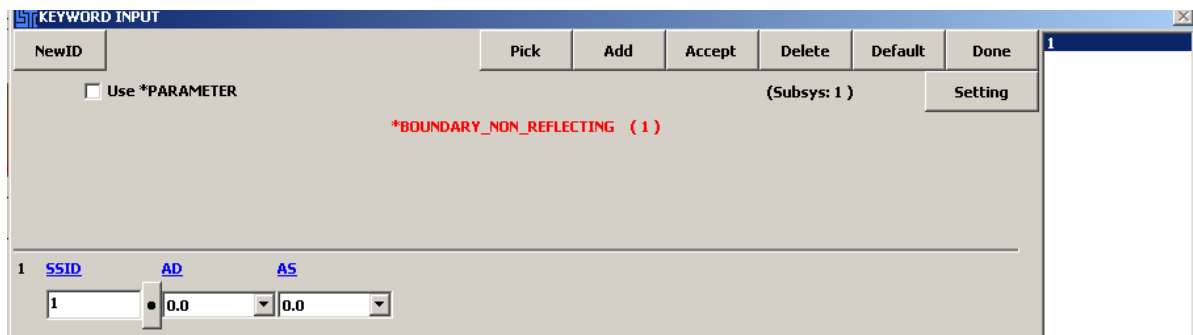


Figure 39 Non-reflecting BC card

STEP 6: Contact Definition

Contact definitions form an integral part of a typical FSI problem. In the present study, the “Constrained-Lagrange-In-Solids” type of Interface/contact is used to model the impact event between the beach/membrane/wavemaker (Lagrangian) and the water-air part sets (Eulerian). Penalty coupling without erosion is used in the present numerical model because the fluid elements are solids and structural ones are shells.

Constrained-Lagrange-In-Solids couples a Lagrangian mesh (slave) of shells to the material points of an Eulerian mesh (master surface). In this, the moving surface of three-dimensional beach/membrane/wavemaker (a Lagrangian mesh) is treated as the slave surface, and the target water-air mesh is treated as the master surface. The slave part or slave part set is coupled to the master part or master part set. The recommended input penalty factor is 0.1. The quadrature rule for coupling slaves to master employs a rectangular grid of 4×4 points. The coupling direction is normal to the structure (wavemaker) and the stress at the interface is compression only.

In addition, all the fluid elements are set up to be an ALE multi-material group so that each element has a specific material property and the ALE formulation tracks the motion of the elements in the numerical simulation. Note that the ALE control settings are essential. In our numerical model, the number of time steps between mesh-smoothing and advection cycles, which could speed up run time but reduce stability, is determined to be unity based on the consideration of computational stability. The first order advection method is applied and it is efficient and accurate for the water. An option is selected (the AFAC value is set at -1) to ensure that no significant element distortion is allowed in the numerical simulation; only expansion and contraction are permitted (LS-DYNA theory manual).

Hence, there is contact between:

Set 1: Wavemaker and Beach (master set) and Air and Water domains (slave set)

Set 2: Membrane structure (master set) and Air and Water domains (slave set)

Figure 36 shows the card details of the contact between the two sets.

Center for Innovation in Ship Design
A Feasibility Study on Numerical Modeling of Large
Scale Naval Fluid Structure: Contact Impact Problems

KEYWORD INPUT

NewID: Pick Add Accept Delete Default Done

☐ Use *PARAMETER (Subsys: 1) Setting

*CONSTRAINED_LAGRANGE_IN_SOLID (2)

COUPID	TITLE
0	
2	
SLAVE	MASTER SSTYPE MSTYP NQUAD CTYPE DIREC MCOUP
2	1 0 0 4 4 2 1
3	START END PFAC FRIC FRCMIN NORM NORMTYP DAMP
0.0	1.000e+010 0.1000000 0.0 0.5000000 0 0 0.0
4	CQ HMIN HMAX ILEAK PLEAK LCIDPOR NVENT BLOCKAGE
0.0	0.0 0.0 0.0 0 0.0100000 0 0 0
5	IBOXID IPENCHK INTFORC IALESEF LAGMUL PFACMM THKE
0	0 0 0 0 0.0 0 0.0

Total Card: 2 Smallest ID: 1 Largest ID: 2 Total deleted card: 0

Figure 40 Constrained Lagrangian in Solid card details

It is important to note that the NQUAD value is set to 4 which determine the number of coupling points assigned to each surface of the Lagrangian elements. In addition, the normal direction of the wavemaker shell elements is very important for the coupling to take place (Figure 37).

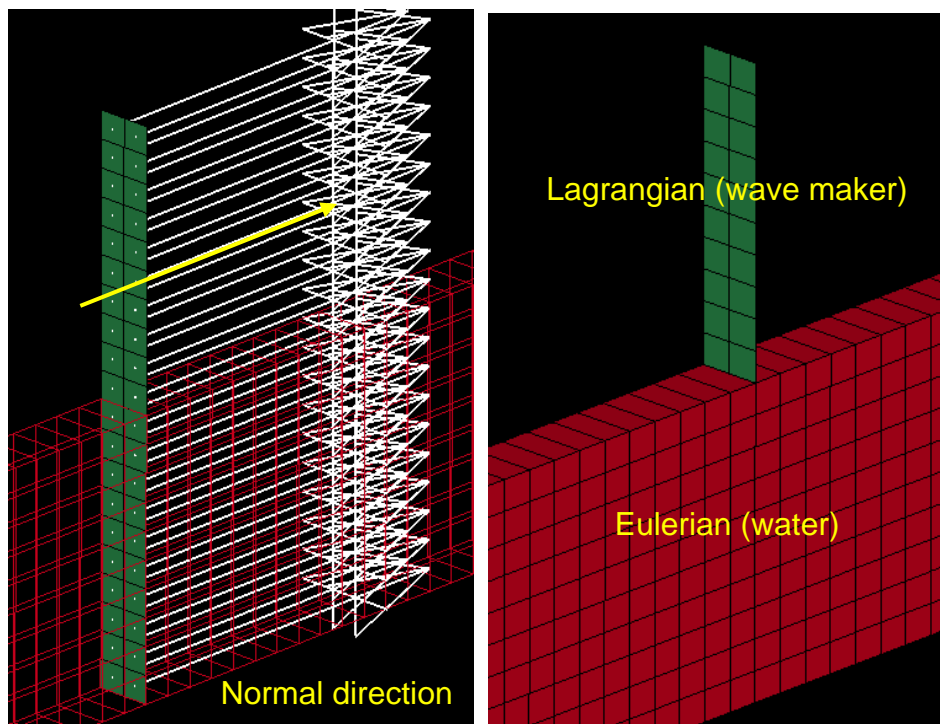


Figure 41 NQUAD/Normal direction of coupling between Lagrangian and Eulerian parts

STEP 7: Defining Curves for Wavemaker Motion and Gravity

➤ Application of Gravity Globally

The gravitation force is applied quasi-statically over a 2-second duration prior to the dynamic simulation and it remains constant throughout the simulation. The value of gravity acceleration is 9.81m/s^2 . Figure 38 shows the graph for the application of gravity. It is however important to mention that in LS-DYNA quasi-static application of gravity is recommended to capture accurate and stable pressure measurements in the water domain (this is the main reason for the variation of gravity from $t=0$ to $t=2\text{sec}$ in the graph shown).

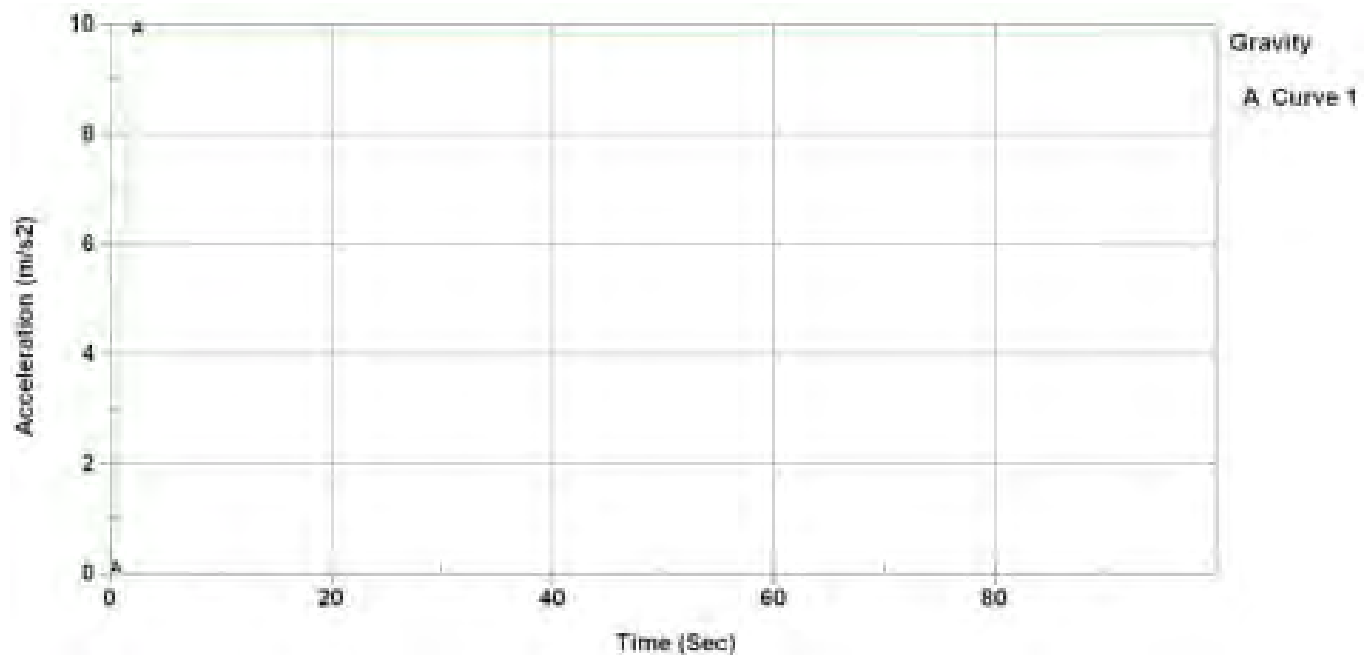


Figure 42 Gravity loading on wave basin (Acceleration time history)

➤ Wavemaker Motion

A piston type wavemaker is used in the current simulation. The stroke of the wavemaker is set at 3" with a frequency of 1Hz. The waves generated are regular waves with simple irregular wave spectra. Figure 39 shows the graph for the wavemaker motion displacement with time. It is important to note that the wavemaker motion starts after gravity has set in properly (i.e., after 2 seconds).

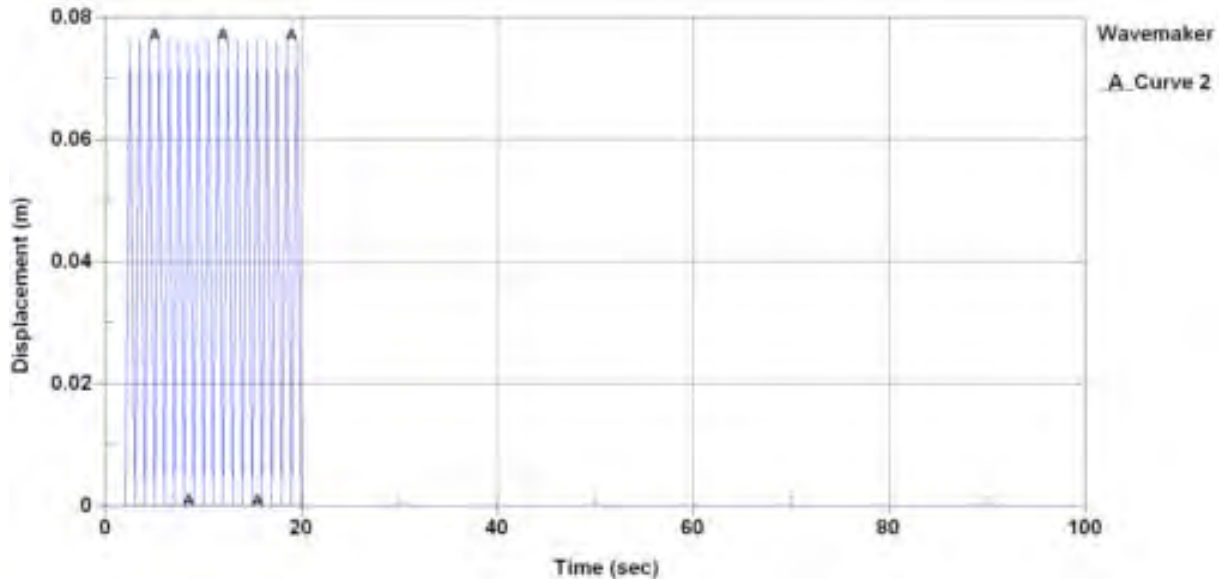


Figure 43 Wavemaker displacement time history

Once the curves for gravity and wavemaker are defined the next step is to assign them independently. The gravity curve is assigned by using the Load_Body_Y option and the wavemaker motion is assigned by used the Boundary Prescribed Motion Rigid card. Figure 40 shows the Load Body card. This card is used to set the gravity force. The Boundary Prescribed Motion Rigid card is used to prescribe the wavemaker motion (Figure 41). Note that the wavemaker moves only in the x-translational direction. VAD is set to 2 which defines the motion in the form of displacement.

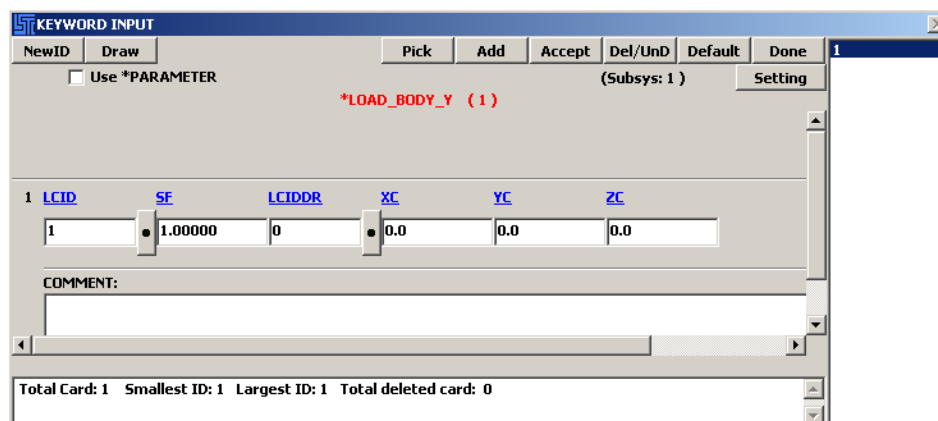
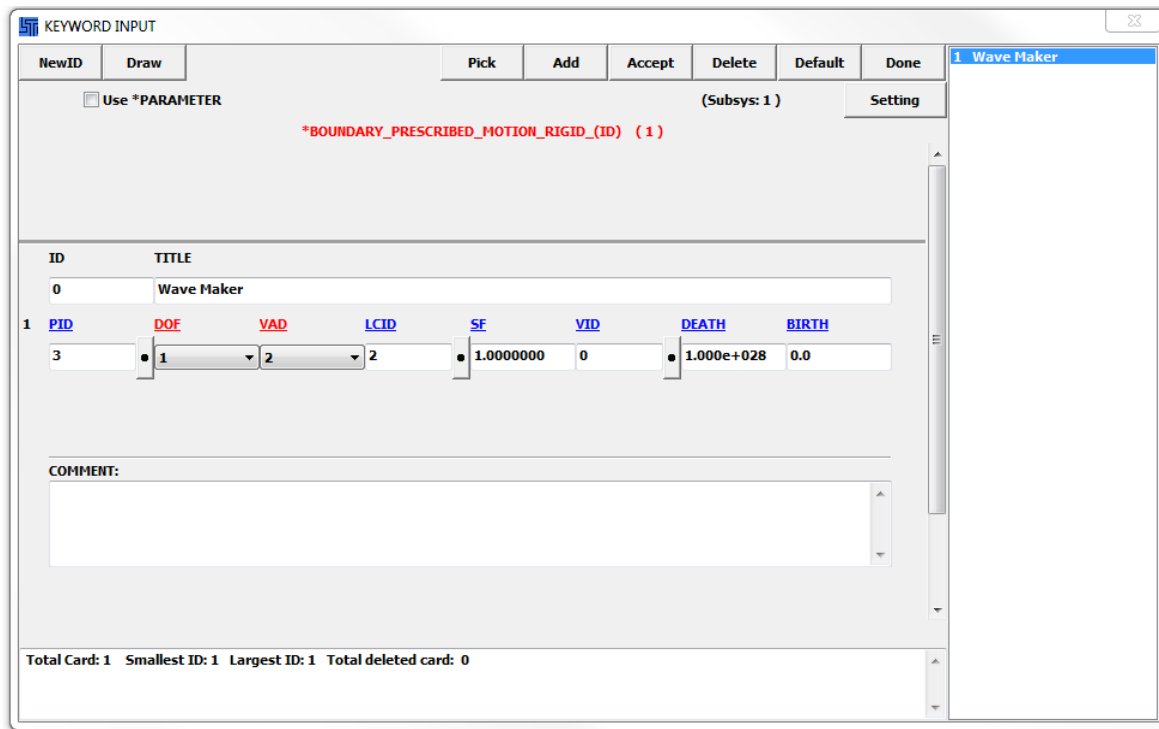


Figure 44 Load Body card to define gravity loading



The screenshot shows a software window titled "KEYWORD INPUT". At the top, there are buttons: "NewID", "Draw", "Pick", "Add", "Accept", "Delete", "Default", and "Done". Below these buttons is a checkbox labeled "Use *PARAMETER" and a label "(Subsys: 1)". A red text label reads "*BOUNDARY_PRESCRIBED_MOTION_RIGID_(ID) (1)". Below this is a table with columns: ID, TITLE, PID, DOF, VAD, LCID, SF, VID, DEATH, and BIRTH. The table contains one row with the following values: ID: 0, TITLE: Wave Maker, PID: 3, DOF: 1, VAD: 2, LCID: 2, SF: 1.0000000, VID: 0, DEATH: 1.000e+028, BIRTH: 0.0. Below the table is a "COMMENT:" label and a text area. At the bottom, a status bar reads "Total Card: 1 Smallest ID: 1 Largest ID: 1 Total deleted card: 0".

ID	TITLE	PID	DOF	VAD	LCID	SF	VID	DEATH	BIRTH
0	Wave Maker	3	1	2	2	1.0000000	0	1.000e+028	0.0

Figure 45 Boundary prescribed motion rigid card for wavemaker motion

➤ Defining Friction Between Beach and Membrane Structure

Figure 42 shows the define friction card between the beach and the membrane structure. As a part of the membrane structure rests on the bottom of the water basin friction has to be defined between the membrane structure and the water basin.

Center for Innovation in Ship Design
A Feasibility Study on Numerical Modeling of Large
Scale Naval Fluid Structure: Contact Impact Problems

KEYWORD INPUT

NewID

Pick

Add

Accept

Delete

Default

Done

2

☐ Use *PARAMETER
 (Subsys: 1)

Setting

*DEFINE_FRICTION (1)

1

ID

FS_D

FD_D

DC_D

VC_D

2

0.0

0.0

0.0

0.0

Repeated Data by Button and List

2

PID_I

PID_I

FS_IJ

FD_IJ

DC_IJ

VC_IJ

5

4

0.000

0.500000

0.000

0.000

1

5

4

0.0000e+000

5.0000e-001

0.0000e+000

0.0000e+000

2

5

2

0.0000e+000

3.0000e-001

0.0000e+000

0.0000e+000

Data Pt. 1

Replace

Insert

Delete

Help

COMMENT:

Total Card: 1

Smallest ID: 2

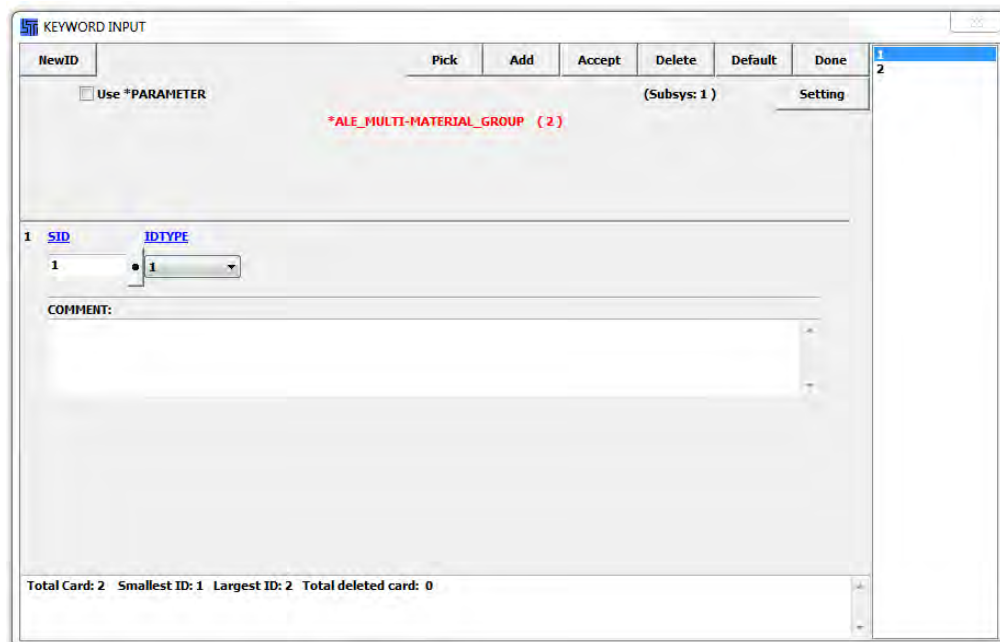
Largest ID: 2

Total deleted card: 0

Figure 46 Friction between membrane structure/beach and bottom of wave basin

STEP 8: Application of ALE Multimaterials

In this model, both the water and air domains are treated as ALE parts so they form an ALE multimaterial set. Figure 43 shows the ALE multimaterial card set definition. In the card shown, “1” stands for the water domain and “2” stands for the air domain.



KEYWORD INPUT

Use *PARAMETER (Subsys: 1) Setting

***ALE_MULTI-MATERIAL_GROUP (2)**

SID	IDTYPE
1	1

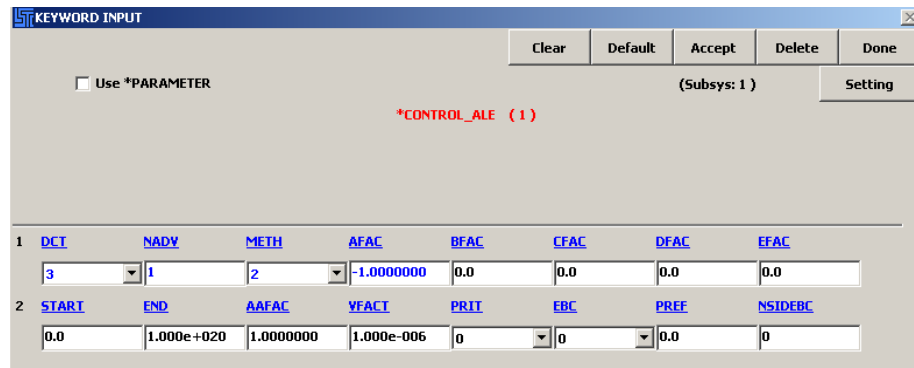
COMMENT:

Total Card: 2 Smallest ID: 1 Largest ID: 2 Total deleted card: 0

Figure 47 Multimaterial ALE card

STEP 9: Control Cards for ALE with Time Step allocation

Control ALE is an important card that defines the type of continuum treatment needed for the ALE formulation along with the method of mesh advection. This card has to be defined whenever and wherever an ALE formulation is used in the numerical simulation. Figure 44 shows the card showing various card values for the control ALE feature. The termination time is set to 10sec-25sec depending on the problem complexity and the time-step is set to 0.9.



1	DCT	NADY	METH	AFAC	BFAC	CFAC	DFAC	EFAC
	3	1	2	-1.0000000	0.0	0.0	0.0	0.0

2	START	END	AAFAC	YFACT	PRIT	EBC	PREF	NSIDEBC
	0.0	1.000e+020	1.0000000	1.000e-006	0	0	0.0	0

Figure 48 Control ALE card details

Details of some of the card parameters are tabulated below.

DCT: Default continuum treatment:

EQ.1: Lagrangian (default)

EQ.2: Eulerian

EQ.3: Arbitrary Lagrangian Eulerian

EQ.4: Eulerian Ambient

METH: Advection method

EQ.1: donor cell + HIS (first order accurate)

EQ.2: Van Leer + half index shift (second order)

EQ.-2 Modified Van Leer

EQ.3: donor cell + HIS, first order accurate, conserving total energy over each advection step instead of conserving internal energy

The time interval between the outputs is defined by using the *Database card. The outputs are in the d3plot format and the “dt” value is set to 0.05 for the current simulation. Finally, check for the duplicate nodes and perform a reference check and see if there are any unassigned card values. Ultimately renumber the node/element/material and section numbers before saving the file.